

CERN-TH/2001-083
March, 2001

Renormalon resummation and exponentiation of soft and collinear gluon radiation in the thrust distribution*

Einan Gardi and Johan Rathsman

TH Division, CERN, CH-1211 Geneva 23, Switzerland

Abstract: The thrust distribution in e^+e^- annihilation is calculated exploiting its exponentiation property in the two-jet region $t = 1 - T \ll 1$. We present a general method (DGE) to calculate a large class of logarithmically enhanced terms, using the dispersive approach in renormalon calculus. Dressed Gluon Exponentiation is based on the fact that the exponentiation kernel is associated primarily with a single gluon emission, and therefore the exponent is naturally represented as an integral over the running coupling. Fixing the definition of Λ is enough to guarantee consistency with the exact exponent to next-to-leading logarithmic accuracy. Renormalization scale dependence is avoided by keeping all the logs. Sub-leading logs, that are usually neglected, are factorially enhanced and are therefore important. Renormalization-group invariance as well as infrared renormalon divergence are recovered in the sum of all the logs. The logarithmically enhanced cross-section is evaluated by Borel summation. Renormalon ambiguity is then used to study power corrections in the peak region $Qt \gtrsim \Lambda$, where the hierarchy between the renormalon closest to the origin ($\sim 1/Qt$) and others ($\sim 1/(Qt)^n$) starts to break down. The exponentiated power-corrections can be described by a shape-function, as advocated by Korchemsky and Sterman. Our calculation suggests that the even central moments of the shape-function are suppressed. Good fits are obtained yielding $\alpha_s^{\overline{\text{MS}}}(M_Z) = 0.110 \pm 0.001$, with a theoretical uncertainty of $\sim 5\%$.

*Research supported in part by the EC program “Training and Mobility of Researchers”, Network “QCD and Particle Structure”, contract ERBFMRXCT980194.

1 Introduction

Event-shape distributions, as well as other observables that are not completely inclusive, tend to have significant contributions from soft and collinear gluon emission. Perturbatively, this appears in the form of logarithmically enhanced terms, the well-known Sudakov logs. Another, more general source of enhancement of perturbative coefficients, which is associated with the running coupling, is infrared renormalons. These appear due to integration over particularly small momenta and therefore reflect the sensitive of the observable to large distance physics. The perturbative expansion of an event-shape distribution has quite a rich structure incorporating both sources of enhancement. Resummation techniques exist for both Sudakov logs and renormalons, separately. Yet, in many cases, both are important. The Dressed Gluon Exponentiation (DGE) method advocated here takes into account both these aspects.

It is understood how infrared renormalons are related to power-corrections through sensitivity to the phase-space boundaries [1]. It is also known that Sudakov logs appear due to the same type of sensitivity [2, 3]. However, the precise relation between the two phenomena was not addressed before, except in the specific case of Drell-Yan production [2, 4], where the emphasis was on the identification of the leading power-correction. DGE allows one to address this relation directly, and thus analyse the distribution in the peak region where the hierarchy between the renormalons starts to break down.

Consider a generic event-shape variable y which is infrared and collinear safe [5], where the limit $y \rightarrow 0$ corresponds to the extreme two-jet configuration. The logarithmically enhanced part of the differential cross-section has the form [6]:

$$\frac{1}{\sigma} \frac{d\sigma}{dy} \Big|_{\log} \sim \frac{1}{y} \sum_{n=1}^{\infty} \sum_{m=0}^{2n-1} c_{n,m} \left(\ln \frac{1}{y} \right)^m a^n, \quad (1)$$

where $a \equiv \alpha_s(Q^2)/\pi$. When $y \ll 1$ a naive fixed-order calculation is not adequate and the large logs must be resummed. However, this does not imply that the full perturbative calculation has to be carried out to all orders: the factorisation of soft and collinear radiation allows one to calculate the log-enhanced part of the cross-section, roughly speaking, “exponentiating the one-loop result”.

It is useful to define the integrated cross-section

$$R(y) \equiv \int_0^y \frac{1}{\sigma} \frac{d\sigma}{dy} dy$$

where the singularity in the two-jet limit, $y \rightarrow 0$, is cancelled by virtual corrections, so that $R(0) = 0$. The logarithmically enhanced part of $R(y)$ has the form $R(y)|_{\log} \sim 1 + \sum_{n=1}^{\infty} R_n(y) a^n$ with

$$R_n(y) = \sum_{m=1}^{2n} r_{n,m} L^m$$

where $L \equiv \ln \frac{1}{y}$ and $r_{n,m} = -c_{n,m-1}/m$. The full $R(y)$ can[†] be written [6] as

$$\ln R(y) = \ln R(y)|_{\log} + \ln R(y)|_{\text{non-log}}, \quad (2)$$

where the first term contains only logarithmic terms that diverge in the two-jet limit whereas the second is finite in this limit.

Exponentiation means that $\ln R(y)|_{\log}$ has the following perturbative expansion,

$$\begin{aligned} \ln R(y)|_{\log} &= \sum_{n=1}^{\infty} \sum_{m=1}^{n+1} G_{n,m} L^m a^n \\ &= L g_1(aL) + g_2(aL) + a g_3(aL) + a^2 g_4(aL) + \dots \end{aligned} \quad (3)$$

where the function $g_1(aL)$ resums the leading-logs (LL) $G_{n,n+1} L^{n+1} a^n$ to all orders, $g_2(aL)$ resums the next-to-leading logs (NLL) $G_{n,n} L^n a^n$, etc. Exponentiation is a universal feature which follows from the factorisation property of QCD matrix elements (see e.g. [7]), provided that the phase-space integration also factorizes. The latter condition makes the calculation of the exact coefficients $G_{n,m}$ rather difficult. However, thanks to an intensive research effort in the last two decades, there is today a detailed understanding of Sudakov logs in a large class of QCD observables. In particular, in the case of event-shape observables in e^+e^- annihilation, like the thrust, the jet mass parameters, the C-parameter, and jet broadening parameters, the state of the art is resummation of $\ln R(y)|_{\log}$ up to NLL accuracy [6, 8, 9].

Current phenomenology of event shape distributions is based on NLL resummation, neglecting $g_k(aL)$ for $k \geq 3$ in (3). The resummed cross-section is matched with next-to-leading order calculations that are available numerically [10, 11]. This combination allows a good qualitative description of the observables, with the main caveat being the fact that “hadronization corrections”, which are not under control theoretically, are required to bridge the gap between the calculation and the measurements.

Before alluding to non-perturbative physics it is worthwhile to re-examine the perturbative calculation. It was already shown in the example of the average thrust, that a major part of the discrepancy between the next-to-leading order calculation and the data can be explained by resummation of higher-order perturbative terms associated with infrared renormalons [12]. Physically the Single Dressed Gluon (SDG) resummation of [12] allows a better description of the branching of a *single* gluon emitted from the primary quark–anti-quark pair. Following the spirit of BLM [13, 14], this resummation takes into account the fact that the physical scale of the emitted gluon is its virtuality, rather than the centre of mass energy Q , which is usually used as the scale of the coupling. As emphasized in [14], the essence of this approach is the idea that the perturbative expansion should be reorganized in a “skeleton expansion” in analogy with the Abelian theory. Then, the separation between running coupling effects and conformal effects is unique and physical. We shall see here, that in the specific context of the Sudakov region, one has access to sub-leading terms in the “skeleton expansion”, corresponding to multiple gluon emission, through exponentiation.

[†]There are various different ways to make this separation. The one we use here is motivated by the so-called log-R matching scheme. See [6].

In order to examine the approximations in the standard NLL perturbative treatment of the thrust distribution, let us first recall two main features of the resummation (3). The first is the fact that the calculation of the functions $g_k(aL)$ is based on an integral over the running coupling. The second is that each $g_k(aL)$ resums a *convergent* series in aL (for $aL \ll 1$). At first sight these facts seem contradictory: usually integrals over the running coupling translate into renormalon factorial divergence. The resolution is that the expansion (3) itself is divergent. The *functions* $g_k(aL)$ increase factorially with k , thus endangering the validity of the truncation at a certain logarithmic accuracy, e.g. NLL. Consequently, when examining the logs $G_{n,m}L^m$ at a fixed order n in eq. (3), one finds that the sub-leading logs are enhanced by a relative factor of $m!$ compared to the leading ones. In the region where the perturbative treatment holds ($aL \ll 1$) this numerical factor can over-compensate the power of the log and thus invalidate the expansion.

Another (related) argument for keeping track of sub-leading logs is the fact that integrals over the running coupling yield at once all powers of L . Therefore, truncation at a certain logarithmic accuracy implies renormalization scheme and scale dependence. A renormalization-group invariant calculation of $\ln R(y)|_{\log}$ requires keeping *all the logs*. Of course, the exact calculation of all the logs is far beyond reach. However, a specific class of logs is fully accessible: these are the logs that are leading in β_0 , $G_{n,m} \sim \beta_0^{n-1}$, namely the ones associated with a single dressed gluon (SDG) emission. Within this class all the sub-leading logs, i.e. the functions $g_k(aL)$, are calculable. Moreover, since the exponentiation kernel is primarily associated with a single gluon, the entire logarithmically enhanced cross-section, which includes any number of gluons, can be generated in some approximation by exponentiating the SDG cross-section. The result is fully consistent with NLL accuracy, provided an adequate choice of the coupling (the “gluon bremsstrahlung” scheme [15]) is made. Our exponentiation procedure is based on the standard assumption that gluons emitted from the primary quark and anti-quark are completely independent and contribute additively to the thrust (this assumption holds for soft gluons). Given this assumption the SDG cross-section exponentiates under the Laplace transform at any logarithmic accuracy. Thus, through integrals over the running coupling we are able to calculate $\ln R(y)|_{\log}$ with the same formal logarithmic accuracy (NLL), yet avoiding any truncation of sub-leading logs, which would inevitably violate renormalization group invariance. In this way we resum at once Sudakov logs and renormalons.

Comparison of the perturbatively calculated event-shape distribution with data requires some phenomenological model to deal with hadronization. Traditionally, hadronization effects are included using detailed Monte-Carlo hadronization models such as HERWIG [16] or PYTHIA [17]. An attractive alternative that became popular recently is to parametrise the effects in terms of a small number of non-perturbative parameters which control power-suppressed contributions. The basic assumption, which we adopt, is that the form of the most important non-perturbative corrections can be deduced from the ambiguities of the perturbative result [18, 19, 20, 21, 22]. It was shown [2, 23, 3] that the primary non-perturbative effect is a shift of the perturbatively calculated distribution to larger values of y :

$$\frac{1}{\sigma} \frac{d\sigma}{dy} \bigg|_{\text{PT}} (y) \longrightarrow \frac{1}{\sigma} \frac{d\sigma}{dy} \bigg|_{\text{PT}} (y - \lambda_1 \Lambda/Q) \quad (4)$$

where λ_1 is a non-perturbative parameter. According to the model of [3], this parameter is expressed as an observable dependent factor which is perturbatively calculable times the “effective infrared coupling” (see [22]). The shift (4) allows a fair description of the data at all measured energies and in a wide range of y values for several event-shapes in terms of a single parameter – the “effective infrared coupling”. The success of this perturbatively motivated approach suggests that the perturbative calculation itself, if pushed further, may be much closer to the data. It should be emphasised though that non-perturbative effects are essential in the two-jet limit when $aL \sim \mathcal{O}(1)$, and in particular in determining the precise location of the distribution peak and its shape. In this region the above-mentioned approach, which uses a single non-perturbative parameter, is insufficient. In [2, 23, 24, 25, 26] a more general approach was suggested, namely to replace the infinite sum of power-corrections of the form $\lambda_n \Lambda^n / (yQ)^n$ which exponentiate by a single shape-function whose central moments are λ_n .

As a consequence of infrared renormalons the resummation of $\ln R(y)|_{\log}$ contains power-suppressed ambiguities which signal the necessity of non-perturbative corrections. The fact that renormalons occur in the exponent strongly suggest that non-perturbative power corrections also exponentiate, in accordance with the shift and the shape-function approaches. We show that the renormalon ambiguity contains valuable information on the non-perturbative corrections, which is not restricted to the level of the leading power correction. In particular, it is possible to deduce the y dependence of each power correction $1/Q^n$ from the corresponding residue of the Borel transform of the exponent. This allows us to make definite predictions concerning the form of the non-perturbative corrections. In the specific case of the thrust distribution the main conclusion from this analysis is that the even central moments of the shape-function are suppressed. Moreover, in the case of the second central moment, an additional cancellation occurs between large-angle contributions, which are included in the shape-function of refs. [25, 26], and a collinear contribution which was not addressed before.

Another important aspect which our approach incorporates is the complementarity between perturbative and non-perturbative contributions, namely renormalon resummation and explicit parametrisation of power corrections [12]. It was clearly shown in [12] that a consistent treatment of non-perturbative power-corrections as well as a reliable determination of α_s requires renormalon resummation. Such resummation is performed here for the first time at the level of the differential cross-section.

This paper deals with a specific observable, the thrust distribution. Nevertheless, DGE is a general method that can be applied in any case where Sudakov logs appear. It makes a direct link between Sudakov resummation and renormalons. This paper is organised as follows: we begin in section 2 by recalling the calculation of the thrust distribution in the single dressed gluon approximation [27]. In principle, this calculation does not require any specific kinematic approximations, however, it is technically simpler if one neglects [15, 12, 27] non-inclusive decay [28] of the gluon into opposite hemispheres. Here we adopt this approximation and provide further evidence for its validity at small values of 1 – thrust. We then observe that log-enhanced terms dominate the single dressed gluon result in a large range of thrust values. This justifies concentrating on the log-enhanced cross-section of the form (1). In section 3 we calculate the resummed

cross-section by exponentiating the logarithmically enhanced part of the SDG result. We also analyse there the renormalon structure of the exponent and the relation with power-correction models mentioned above. In section 4 we compare our approach with the calculation of [6] which is based on solving an evolution equation for the jet mass distribution. In particular we show that the two calculations coincide up to NLL accuracy, provided an appropriate choice of the coupling is made [15]. In section 5 we study the phenomenological implication of the suggested resummation by fitting to data in a large range of energies and in section 6 we summarise our conclusions.

2 Thrust distribution from Single Dressed Gluon

The purpose of this section is to calculate the thrust distribution in case of a single gluon emission. The result will be used in section 3 to calculate the physical multi-gluon cross-section, through exponentiation. We begin by recalling the calculation of the Single Dressed Gluon characteristic function (sec. 2.1). Then, in sec. 2.2, we isolate the logarithmically enhanced terms and study their structure and finally, in sec 2.3, we construct the Borel representation of the result.

2.1 Single Dressed Gluon (SDG) characteristic function

In renormalon calculations [1, 22] the all-order perturbative result, which resums all the terms that are leading in β_0 , can be expressed as a time-like momentum integral of an observable dependent Single Dressed Gluon (SDG) characteristic function, times an observable independent effective-charge:

$$\int_0^\infty \frac{d\epsilon}{\epsilon} \dot{\mathcal{F}}(\epsilon) \bar{A}_{\text{eff}}(\epsilon Q^2) = \int_0^\infty \frac{d\epsilon}{\epsilon} [\mathcal{F}(\epsilon) - \mathcal{F}(0)] \bar{\rho}(\epsilon Q^2) \quad (5)$$

where $\bar{A}(k^2) \equiv \beta_0 \bar{a}(k^2) = \beta_0 \bar{\alpha}_s(k^2)/\pi$, and the bar stands for a specific renormalization-scheme. In the large β_0 limit (large N_f limit) $\bar{A}(k^2)$ is related to the $\overline{\text{MS}}$ coupling $A(k^2) \equiv \beta_0 \alpha_s^{\overline{\text{MS}}}(k^2)/\pi$ by

$$\bar{A}(k^2) = \frac{A(k^2)}{1 - \frac{5}{3}A(k^2)}. \quad (6)$$

Going beyond this limit is discussed in sec. 4. The two integrals in (5) are related by integration by parts:

$$\dot{\mathcal{F}}(\epsilon) \equiv -\epsilon \frac{d}{d\epsilon} \mathcal{F}(\epsilon), \quad (7)$$

and the function $\bar{\rho}(\mu^2)$ is identified as the time-like discontinuity of the coupling,

$$\bar{\rho}(\mu^2) = \frac{1}{2\pi i} \text{Disc} \left\{ \bar{A}(-\mu^2) \right\} \equiv \frac{1}{2\pi i} \left[\bar{A}(-\mu^2 + i\epsilon) - \bar{A}(-\mu^2 - i\epsilon) \right]. \quad (8)$$

The “time-like coupling” $\bar{A}_{\text{eff}}(\mu^2)$ in (5) obeys

$$\mu^2 \frac{d\bar{A}_{\text{eff}}(\mu^2)}{d\mu^2} = \bar{\rho}(\mu^2). \quad (9)$$

For example, in the one-loop case $\bar{A}(k^2) = 1/(\ln k^2/\bar{\Lambda}^2)$ and

$$\bar{A}_{\text{eff}}(\mu^2) = \frac{1}{2} - \frac{1}{\pi} \arctan \left(\frac{1}{\pi} \ln \frac{\mu^2}{\bar{\Lambda}^2} \right). \quad (10)$$

The characteristic function $\mathcal{F}(\epsilon)$ itself can be calculated either using the Abelian large N_f limit followed by naive non-Abelianization [1], or in the dispersive approach [22], referring to $\mu^2 = \epsilon Q^2$ as the squared gluon mass. In case of inclusive observables, such as the total cross-section in e^+e^- annihilation, the two calculations coincide. The two differ [28, 22, 12, 27, 26], however, in the case of observables such as event-shape variables, that are not completely inclusive with respect to the decay products of the gluon. Here we shall use the massive-gluon characteristic function for the thrust distribution, which was calculated in [27]. It corresponds to an inclusive integration over the decay products of the gluon, so that the possibility that a gluon decays into partons that end up in opposite hemispheres is not taken into account. It is important to emphasise, though, that the steps that follow can be repeated in very much the same way starting with the large N_f result, once available. In the case of the thrust, the inclusive approximation is expected to be good (some evidence is given below). Note that for some event-shapes, e.g. the heavy jet mass, this is probably not so.

Let us now briefly recall the calculation of the thrust distribution characteristic function of ref. [27]. At the SDG level, the distribution of $t = 1 - \text{thrust}$ is

$$\frac{1}{\sigma} \frac{d\sigma}{dt}(Q^2, t) \Big|_{\text{SDG}} = \frac{C_F}{\beta_0} \int_0^1 \frac{d\epsilon}{\epsilon} \bar{A}_{\text{eff}}(\epsilon Q^2) \dot{\mathcal{F}}(\epsilon, t) = \frac{C_F}{\beta_0} \int_0^1 \frac{d\epsilon}{\epsilon} \bar{\rho}(\epsilon Q^2) [\mathcal{F}(\epsilon, t) - \mathcal{F}(0, t)]. \quad (11)$$

The characteristic function $\mathcal{F}(\epsilon, t)$ is obtained from the following integral over phase-space,

$$\mathcal{F}(\epsilon, t) = \int_{\text{phase space}} dx_1 dx_2 \mathcal{M}(x_1, x_2, \epsilon) \delta(1 - T(x_1, x_2, \epsilon) - t) \quad (12)$$

where $C_F a \mathcal{M}$ is the squared tree level matrix element for the production of a quark-anti-quark pair and a gluon of virtuality $\mu^2 \equiv \epsilon Q^2$, and

$$\mathcal{M}(x_1, x_2, \epsilon) = \frac{1}{2} \left[\frac{(x_1 + \epsilon)^2 + (x_2 + \epsilon)^2}{(1 - x_1)(1 - x_2)} - \frac{\epsilon}{(1 - x_1)^2} - \frac{\epsilon}{(1 - x_2)^2} \right]. \quad (13)$$

The integration variables $x_{1,2}$ represent the energy fraction of each of the quarks in the centre-of-mass frame. The energy fraction of the gluon is $x_3 = 2 - x_1 - x_2$.

We use the following [22, 12, 27] definition of the thrust

$$T = \frac{\sum_i |\vec{p}_i \cdot \vec{n}_T|}{\sum_i E_i} = \frac{\sum_i |\vec{p}_i \cdot \vec{n}_T|}{Q}. \quad (14)$$

In case of three partons (a quark, an anti-quark and a “massive” gluon) it yields [12],

$$1 - T(x_1, x_2, \epsilon) = \min \left\{ 1 - x_1, 1 - x_2, 1 - \sqrt{(2 - x_1 - x_2)^2 - 4\epsilon} \right\}. \quad (15)$$

Evaluating (12) one obtains [27] the characteristic function for the thrust distribution,

$$\mathcal{F}(\epsilon, t) = \begin{cases} \mathcal{F}_Q^l(\epsilon, t) + \mathcal{F}_G(\epsilon, t) & \epsilon < t < \sqrt{\epsilon} \\ \mathcal{F}_Q^h(\epsilon, t) + \mathcal{F}_G(\epsilon, t) & \sqrt{\epsilon} < t < \frac{2}{3}\sqrt{1+3\epsilon} - \frac{1}{3} \end{cases} \quad (16)$$

where the dominant contribution $\mathcal{F}_Q(\epsilon, t)$ corresponds to the phase-space regions where one of the primary quarks carries the largest momentum ($T = x_{1,2}$) and $\mathcal{F}_G(\epsilon, t)$ corresponds to the region where the gluon momentum is the largest. The superscripts l and h on $\mathcal{F}_Q(\epsilon, t)$ denote low and high t values, respectively. These functions are given by

$$\begin{aligned} \mathcal{F}_Q^h(\epsilon, t) &= -\frac{1}{t} \left[(1-t+\epsilon)^2 + (1+\epsilon)^2 \right] \ln \frac{t}{q-t} + \left(3 - 2 \frac{q}{t} + \frac{1}{2} \frac{1}{t} + \frac{1}{2} t - q \right) \\ &+ \left(4 - 2 \frac{q}{t} + 3 \frac{1}{t} - \frac{q}{t^2} + \frac{1}{q-t} \right) \epsilon \\ \mathcal{F}_Q^l(\epsilon, t) &= -\frac{1}{t} \left[(1-t+\epsilon)^2 + (1+\epsilon)^2 \right] \ln \frac{\epsilon}{t(q-t)} + \left(1 - 2 \frac{q}{t} + \frac{1}{2} \frac{1}{t} - q \right) \\ &+ \left(3 \frac{1}{t} + \frac{1}{q-t} - \frac{q}{t^2} + 2 \frac{1}{t^2} + 2 - 2 \frac{q}{t} \right) \epsilon + \left(2 + \frac{1}{2t} \right) \frac{\epsilon^2}{t^2} \\ \mathcal{F}_G(\epsilon, t) &= \frac{1-t}{q^2} \left[\left((1+\epsilon)^2 + (1+\epsilon-q)^2 \right) \ln \frac{q-t}{t} + (2t-q) \left(q + \frac{\epsilon}{t} + \frac{\epsilon}{q-t} \right) \right] \end{aligned} \quad (17)$$

where $q \equiv \sqrt{(1-t)^2 + 4\epsilon}$.

2.2 Logarithmically Enhanced Terms

Next we examine the SDG perturbative expression (11) with the characteristic function of eqs. (16) and (17). For this purpose it is convenient to expand the time-like coupling $\bar{A}_{\text{eff}}(\epsilon Q^2)$ in terms of a fixed-scale space-like coupling $\bar{A}(Q^2)$,

$$\bar{A}_{\text{eff}}(\epsilon Q^2) = \sum_{m=0}^{\infty} \left(\bar{A}(Q^2) \right)^{m+1} \sum_{j=0}^m K_{m,j} \left(\ln \frac{1}{\epsilon} \right)^j, \quad (18)$$

where, in general, $K_{m,j}$ depend on the coefficients of the β function which controls the evolution of $\bar{A}(Q^2)$. Performing the integral (11) over $\dot{\mathcal{F}}(\epsilon, t) \equiv -\epsilon \frac{d}{d\epsilon} \mathcal{F}(\epsilon, t)$ order by order one gets the sum

$$\frac{1}{\sigma} \frac{d\sigma}{dt}(Q^2, t) \Big|_{\text{SDG}} = \frac{C_F}{\beta_0} \sum_{m=0}^{\infty} \left(\bar{A}(Q^2) \right)^{m+1} \sum_{j=0}^m K_{m,j} h_j(t) \quad (19)$$

where the functions $h_j(t)$ are the log-moments of the characteristic function,

$$h_j(t) = \int_0^1 \frac{d\epsilon}{\epsilon} \left(\ln \frac{1}{\epsilon} \right)^j \dot{\mathcal{F}}(\epsilon, t). \quad (20)$$

The analytic calculation of $h_j(t)$ with the full characteristic function of eqs. (16) and (17) is rather involved. Alternatively, concentrating in the small t region, we distinguish in

$h_j(t)$ between logarithmically enhanced terms which are not suppressed by any power of t and the rest, which we eventually neglect.

As we shall see, the logarithmically enhanced terms, which have the form of eq. (1), can be easily computed analytically to all orders. Using (16) for $t < 1/3$ we obtain

$$h_j(t) = \int_0^t \frac{d\epsilon}{\epsilon} \left(\ln \frac{1}{\epsilon} \right)^j \dot{\mathcal{F}}_G(\epsilon, t) + \int_0^{t^2} \frac{d\epsilon}{\epsilon} \left(\ln \frac{1}{\epsilon} \right)^j \dot{\mathcal{F}}_Q^h(\epsilon, t) + \int_{t^2}^t \frac{d\epsilon}{\epsilon} \left(\ln \frac{1}{\epsilon} \right)^j \dot{\mathcal{F}}_Q^l(\epsilon, t). \quad (21)$$

We notice that a term of the form ϵ^n/t^k in $\dot{\mathcal{F}}(\epsilon, t)$ contributes to $h_j(t)$ a term proportional to t^{n-k} (times a polynomial in $\ln \frac{1}{t}$) from the collinear gluon emission limit of phase-space[‡] where $\epsilon = t$, and a term proportional to t^{2n-k} (times a polynomial in $\ln \frac{1}{t}$) from the large-angle soft gluon emission limit of phase-space where $\epsilon = t^2$. Taking the double expansion of (17) at small t and ϵ we have

$$\begin{aligned} \dot{\mathcal{F}}_Q^h(\epsilon, t) &\simeq \frac{\epsilon}{t^2} + \frac{\mathcal{O}(\epsilon)}{t} \\ \dot{\mathcal{F}}_Q^l(\epsilon, t) &\simeq -\frac{\epsilon^2}{t^3} - \frac{\epsilon}{t^2} + \frac{2}{t} + \mathcal{O}(1) \\ \dot{\mathcal{F}}_G(\epsilon, t) &\simeq \frac{\epsilon}{t} + \mathcal{O}(1) \end{aligned} \quad (22)$$

where we ignored higher powers of ϵ multiplying a given power of $1/t$, which are not relevant. From (21) and (22) we conclude that only $\dot{\mathcal{F}}_Q^l(\epsilon, t)$ contributes to the logarithmically enhanced cross-section and thus

$$h_j(t)|_{\log} = \int_{t^2}^t \frac{d\epsilon}{\epsilon} \left(\ln \frac{1}{\epsilon} \right)^j \left[-\frac{\epsilon^2}{t^3} - \frac{\epsilon}{t^2} + \frac{2}{t} \right]. \quad (23)$$

Performing the integral over ϵ yields

$$\begin{aligned} h_j(t)|_{\log} &= \frac{1}{t} \left[2 \frac{2^{j+1} - 1}{j+1} L^{j+1} - e^L \Gamma(j+1, L) - 2^{-j-1} e^{2L} \Gamma(j+1, 2L) \right] \\ &= \frac{1}{t} \left[2 \frac{2^{j+1} - 1}{j+1} L^{j+1} - \sum_{k=0}^j \frac{j!}{k!} (1 + 2^{k-j-1}) L^k \right] \end{aligned} \quad (24)$$

where $L \equiv \ln \frac{1}{t}$.

Having evaluated the log-moments we can substitute them into (19) to obtain the logarithmically enhanced SDG differential cross-section to arbitrarily high order. The result (24) has a few features that deserve attention. First we note that the leading-logs in $h_j(t)$ depend on both collinear and large-angle soft gluon limits of phase-space, while the sub-leading logs are associated with the collinear limit alone. Next, we observe that the leading-logs in $h_j(t)$ originate in the ϵ independent term $2/t$ in $\dot{\mathcal{F}}_Q^l(\epsilon, t)$, while the sub-leading logs originate in the two ϵ dependent terms, $-\epsilon^2/t^3 - \epsilon/t^2$. This ϵ dependence is reflected in factorial increase of the coefficients (see below) which is associated with the sensitivity of the thrust to collinear gluon emission.

[‡]A detailed analysis of the phase-space can be found in [27]. See figure 1 there.

It is important to notice that the factorial growth is associated with sub-leading logs. Considering the different logs L^k in a given log-moment $h_j(t)$ we find that with decreasing power k the numerical coefficient increases as $j!/k!$. Note, in particular, that the next-to-leading logs L^j (which are the only sub-leading logs taken into account in the standard analysis) have a small coefficient ($\frac{3}{2}$), while further sub-leading logs (which are usually ignored) are multiplied by large numbers. It is useful to analyse the square brackets in (24) by considering two extreme limits for the function $F(L) \equiv e^L \Gamma(j+1, L)$. In the limit $L \rightarrow 0$, one finds factorial growth $F(L) \sim j!$. In the limit $L \rightarrow \infty$ one can keep only the leading logarithmic term in $F(L)$, i.e. $F(L) \sim L^j$, recovering the standard NLL result. The fact that the latter formally holds may be of little relevance in practice given that the entire perturbative treatment is adequate only when $L \ll 1/\bar{A}(Q^2)$. One can now examine the validity of these two extreme approximations for phenomenologically interesting values of L . Consider for example the case $t = 0.05$, $L = \ln(1/0.05) \simeq 3$ at order $j = 3$: the value is $F(L) = 77.8$ while the NLL gives $L^j = 26.9$ and the naive factorial gives $j! = 6$. Clearly, none of these extreme approximations is valid. One must retain all the logs.

One may wonder to what extent it is justified to consider only the logarithmically enhanced part of the log moments. Factorial increase is certainly not restricted to the logarithmically enhanced part. The immediate answer is, of course, that the neglected part is parametrically smaller, by a factor of t compared to the one kept. This answer is not complete: as we know, parametric suppression can be compensated by large numerical coefficients. To be convinced that this approximation is valid at physically interesting values of t let us now compare the logarithmic part of the log-moments $h_j(t)$ with the full function which we evaluate numerically. Writing $h_j(t) = h_j(t)|_{\log} + \Delta h_j(t)$, where the logarithmically enhanced part $h_j(t)|_{\log}$ is given by (24) and $\Delta h_j(t)$ are suppressed by a relative factor of t , the first few log-moments are

$$\begin{aligned} h_1(t) &= \frac{1}{t} \left[3L^2 - \frac{3}{2}L - \frac{5}{4} + \Delta h_1(t) \right] \\ h_2(t) &= \frac{1}{t} \left[\frac{14}{3}L^3 - \frac{3}{2}L^2 - \frac{5}{2}L - \frac{9}{4} + \Delta h_2(t) \right] \\ h_3(t) &= \frac{1}{t} \left[\frac{15}{2}L^4 - \frac{3}{2}L^3 - \frac{15}{4}L^2 - \frac{27}{4}L - \frac{51}{8} + \Delta h_3(t) \right] \\ h_4(t) &= \frac{1}{t} \left[\frac{62}{5}L^5 - \frac{3}{2}L^4 - 5L^3 - \frac{27}{2}L^2 - \frac{51}{2}L - \frac{99}{4} + \Delta h_4(t) \right] \end{aligned}$$

The $h_j(t)$ and thus $\Delta h_j(t)$ are calculated by integrating (20) numerically where $\dot{\mathcal{F}}(\epsilon, t)$ is the derivative of the *full* characteristic function (17). The comparison for the first four log-moments is presented in fig. 1. We see that while the NLL approximation is quite far from the actual values of $h_j(t)$ even at rather small t , there is a fairly wide range in which the logarithmic approximation $h_j(t)|_{\log}$ is good. At large t values the gap between the two increases. However, since our interest here is in improving the calculation in the small t region, we consider this agreement satisfactory. It should be kept in mind, though, that our resummation procedure is not the appropriate way to improve the calculation of the cross-section at $t \gtrsim 0.2$. We comment that for higher log-moments $j \geq 5$ the

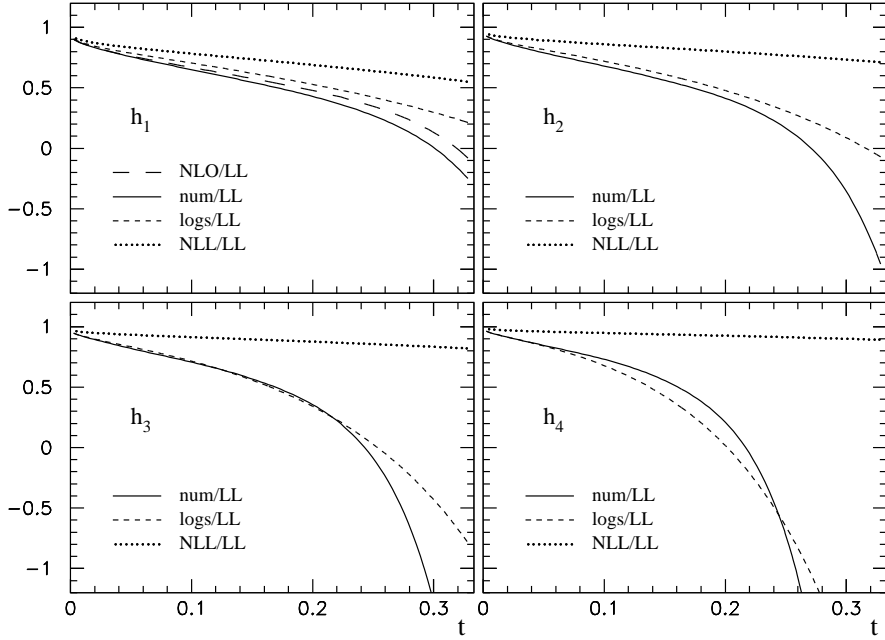


Figure 1: The functions $h_j(t)$, $j = 1$ through 4, in different approximations normalised to the leading logarithm (LL). The complete result (calculated numerically) is the full line and the sum of the logarithmically enhanced terms $h_j(t)|_{\log}$ (calculated analytically) is dashed, the NLL approximation is dotted. For the first moment, the β_0 dependent part of the NLO result is also shown for comparison.

approximation deteriorates even at smaller t values; however, the resulting discrepancy at the level of the SDG cross-section (19) is not large. We shall revisit the significance of terms that are suppressed by t in the phenomenological analysis in sec. 5.

Finally, using (6), the first few orders of the SDG calculation (19) of the log-enhanced cross-section are given in the $\overline{\text{MS}}$ scheme by

$$\begin{aligned} \frac{1}{\sigma} \frac{d\sigma}{dt}(Q^2, t) \Big|_{\text{SDG}} &= \frac{C_F}{t \beta_0} \left\{ (2L - 1.5) A(Q^2) + (3L^2 + 1.8333L - 3.75) A(Q^2)^2 \right. \\ &+ (4.6667L^3 + 8.5000L^2 - 8.5242L - 5.6481) A(Q^2)^3 \\ &+ (7.5000L^4 + 21.833L^3 - 15.859L^2 - 40.585L + 2.025) A(Q^2)^4 \\ &\left. + (12.400L^5 + 48.500L^4 - 29.339L^3 - 175.72L^2 - 47.164L + 40.22) A(Q^2)^5 + \dots \right\} \end{aligned} \quad (25)$$

The leading and next-to-leading logs are consistent with previous calculations [6]. In addition, at NLO we can compare the next-to-next-to-leading log (-3.75 in (25)) with the exact numerical computation [11]. To make an explicit comparison, one should separate the contributions of different colour factors in the NLO coefficient (this was done before in [38]) and then fit the numerical results to a parametric form which includes a log-enhanced part, and terms which are suppressed by powers of t . The result of such a fit,

where the first two logs are fixed to their exact values, gives the following log-enhanced NLO expression in the large β_0 limit,

$$\frac{1}{\sigma} \frac{d\sigma}{dt}(Q^2, t) \Big|_{\text{NLO}} = \frac{C_F}{t \beta_0} \left\{ (2L - 1.5) A(Q^2) + (3L^2 + 1.8333L - 3.77 \pm 0.07) A(Q^2)^2 \right\}. \quad (26)$$

Details concerning the fit and the error estimate can be found in the Appendix. The closeness of the NNLL coefficients is encouraging. It strongly suggests that the impact of the non-inclusive splitting of the gluon into partons that end up in opposite hemispheres [28], which is not taken into account in our calculation, is small, at least at the logarithmic level. A similar comparison, which goes beyond the logarithmic level, has been performed for the average thrust in [12, 27] and the higher moments $\langle t^n \rangle$ in [27]. It was found that the non-inclusive effect is rather small for the average thrust (4.4%) while it increases for the higher moments. This implies that the effect is mainly important in the large t region. Being interested here in the small t region and in particular in the logarithmically enhanced part of the cross section, we shall neglect this effect altogether. The reader should keep in mind, however, that the evidence provided above concerns directly only the Abelian part of the coefficients. Only through the assumption that running coupling effects dominate (making the large β_0 approximation legitimate) this evidence becomes relevant for the non-Abelian non-inclusive effect. Moreover, in the context of power-corrections within the infrared-finite coupling approach, the impact of the non-inclusive effect in the non-Abelian case was shown to be more significant than in the Abelian one [32, 33].

2.3 Borel representation of the SDG result

A convenient way to deal with perturbation theory to all orders is Borel summation. In this section we construct the scheme-invariant Borel representation of the logarithmically enhanced part of the SDG result. This will be used in the next section to calculate the multiple emission cross-section. We start with the scheme-invariant Borel representation of the coupling [29, 30, 31],

$$\bar{A}(k^2) = \int_0^\infty dz \exp(-z \ln k^2/\Lambda^2) \bar{A}_B(z). \quad (27)$$

In the case of one-loop running coupling $\bar{A}_B(z) = \exp(-z \ln \Lambda^2/\bar{\Lambda}^2)$. Taking the time-like discontinuity [29] we get

$$\bar{A}_{\text{eff}}(Q^2) = \int_0^\infty dz \exp(-z \ln Q^2/\Lambda^2) \frac{\sin \pi z}{\pi z} \bar{A}_B(z). \quad (28)$$

In eq. (11) we use the part of $\dot{\mathcal{F}}(\epsilon, t)$ that contributes to log-enhanced terms (as in (23)),

$$\frac{1}{\sigma} \frac{d\sigma}{dt}(Q^2, t) \Big|_{\text{SDG}} = \frac{C_F}{\beta_0} \int_{t^2}^t \frac{d\epsilon}{\epsilon} \bar{A}_{\text{eff}}(\epsilon Q^2) \left[-\frac{\epsilon^2}{t^3} - \frac{\epsilon}{t^2} + \frac{2}{t} \right]. \quad (29)$$

Substituting $\bar{A}_{\text{eff}}(\epsilon Q^2)$ from (28) and integrating over ϵ we obtain the Borel representation of the logarithmically enhanced SDG cross-section,

$$\frac{1}{\sigma} \frac{d\sigma}{dt}(Q^2, t) \Big|_{\text{SDG}} = \frac{C_F}{\beta_0} \frac{1}{t} \int_0^\infty dz B_{\text{SDG}}(z, t) \exp\left(-z \ln Q^2/\Lambda^2\right) \frac{\sin \pi z}{\pi z} \bar{A}_B(z) \quad (30)$$

with

$$B_{\text{SDG}}(z, t) = \frac{2}{z} \exp(2zL) - \left(\frac{2}{z} + \frac{1}{1-z} + \frac{1}{2-z} \right) \exp(zL) \quad (31)$$

where $L \equiv \ln \frac{1}{t}$. Note that the first exponent in the Borel transform is associated with the large-angle soft gluon limit of phase-space, while the second is associated with the collinear limit. The Borel integral is well-defined at the perturbative level thanks to the cancellation of the pole at $z = 0$ between these two contributions. Moreover, provided that the coupling does not enhance the singularity (e.g. the case of one-loop coupling), the poles at $z = 1$ and $z = 2$ are regulated by the $\frac{\sin \pi z}{\pi z}$ factor, which originates in the analytic continuation to the time-like region.

Note that the Borel integral converges at infinity only provided that $2L < \ln Q^2/\bar{\Lambda}^2$, or $Qt > \bar{\Lambda}$, reflecting large-angle gluon emission sensitivity. A weaker condition appears from the collinear limit: $L < \ln Q^2/\bar{\Lambda}^2$, or $Q^2 t > \bar{\Lambda}^2$. These convergence conditions signal the fact that the small t region is not under control in perturbation theory, and that power corrections of the form $\Lambda^n/(Qt)^n$ (and eventually also $\Lambda^{2n}/(Q^2 t)^n$) should be included [20, 25, 26]. We will return to this point in more detail in the next section.

3 Exponentiation

The calculation of the previous section concerns a *single* gluon emission from the primary quark–anti-quark pair. Close to the two-jet limit, resummation of multiple soft and collinear gluons is essential. This resummation is achieved by exponentiating the SDG cross-section. As mentioned in the introduction, our basic assumption is that emission of several soft or collinear gluons can be regarded as independent. The total contribution to the thrust is then computed as the sum of the individual contributions of these emissions: $t = \sum_{k=1}^n t_k$. For large-angle soft gluons, which give the dominant contribution at small t , additivity holds since the contribution of each gluon to t is proportional to its transverse momentum. This assumption fails, of course, for sufficiently hard gluons. In general, the contribution of several gluons to the thrust, as any other event-shape, are *correlated*. Such a correlation emerges from the modification of the phase-space limits in the integration over the gluon momenta (the quarks do recoil) as well as from additional interactions between the emitted gluons. These correlations are expected to be important only at large values of $1 - \text{thrust}$, away from the two-jet configuration. Since they may have an effect at the logarithmic level, our calculation of sub-leading logs (beyond NLL accuracy) that are sub-leading in β_0 [§] is only partial. It remains for future work to quantify the effect of these correlations. Here we simply assume that it is small.

[§]Such correlations do not affect the logs that are leading in β_0 . These terms are not modified by the exponentiation and their calculation in the previous section is exact barring the inclusive approximation made in the definition of the thrust.

3.1 Exponentiation Formula

The result of the previous section, $\frac{1}{\sigma} \frac{d\sigma}{dt}(Q^2, t) \Big|_{\text{SDG}}$, has a probabilistic interpretation as the probability distribution, of the random variable $t \in (0, 1)$, given that only one gluon is emitted. Since, in reality any number of gluons n can be emitted, we sum over these possibilities

$$\frac{1}{\sigma} \frac{d\sigma}{dt}(Q^2, t) \Big|_{\text{res}} = \sum_{n=0}^{\infty} \frac{1}{n!} \prod_{k=1}^n \int_0^1 \frac{1}{\sigma} \frac{d\sigma}{dt}(t_k) \Big|_{\text{SDG}} dt_k \left[\delta \left(t - \sum_{k=1}^n t_k \right) - \delta(t) \right] \quad (32)$$

where the singularity due to zero gluon emission probability $n = 0$ is cancelled by virtual corrections, $\delta(t)$. The combinatorial $n!$ is introduced to avoid multiple counting – the expression is symmetric for any permutation of the n gluons. Using the Laplace conjugate variable ν , the δ function can be written in a factorized form as (see e.g. [20]),

$$\delta(t - \sum_{k=1}^n t_k) = \int_{\mathcal{C}} \frac{d\nu}{2\pi i} \exp \left\{ -\nu \left(\sum_{k=1}^n t_k - t \right) \right\}. \quad (33)$$

where the contour \mathcal{C} runs parallel to the imaginary axis (to the right of all the singularities of the integrand, if any). Changing the order of the ν integration and the sum over n in (32) we get the exponentiated form,

$$\begin{aligned} \frac{1}{\sigma} \frac{d\sigma}{dt}(Q^2, t) \Big|_{\text{res}} &= \int_{\mathcal{C}} \frac{d\nu}{2\pi i} e^{\nu t} \sum_{n=0}^{\infty} \frac{1}{n!} \left[\int_0^1 \frac{1}{\sigma} \frac{d\sigma}{dt}(t_k) \Big|_{\text{SDG}} (e^{-\nu t_k} - 1) dt_k \right]^n \\ &= \int_{\mathcal{C}} \frac{d\nu}{2\pi i} e^{\nu t} \exp \left\{ \int_0^1 \frac{1}{\sigma} \frac{d\sigma}{dt}(Q^2, t) \Big|_{\text{SDG}} (e^{-\nu t} - 1) dt \right\} \end{aligned} \quad (34)$$

Defining

$$\mathcal{S}_{\text{PT}}(Q^2, \ln \nu) \equiv \left\langle e^{-\nu t} \right\rangle_{\text{SDG}} \equiv \int_0^1 \frac{1}{\sigma} \frac{d\sigma}{dt}(Q^2, t) \Big|_{\text{SDG}} (e^{-\nu t} - 1) dt, \quad (35)$$

we have

$$\frac{1}{\sigma} \frac{d\sigma}{dt}(Q^2, t) \Big|_{\text{res}} = \int_{\mathcal{C}} \frac{d\nu}{2\pi i} e^{\nu t} \exp \left\{ \left\langle e^{-\nu t} \right\rangle_{\text{SDG}} \right\}, \quad (36)$$

and finally, integrating over t ,

$$R(Q^2, t) \Big|_{\text{res}} = \int_{\mathcal{C}} \frac{d\nu}{2\pi i} \nu e^{\nu t} \exp \left\{ \left\langle e^{-\nu t} \right\rangle_{\text{SDG}} \right\}. \quad (37)$$

Note that the terms which are leading in β_0 in the coefficients of $\frac{1}{\sigma} \frac{d\sigma}{dt}(Q^2, t) \Big|_{\text{res}}$, or in the log-enhanced part of the exact result, are the *same* as the ones in $\frac{1}{\sigma} \frac{d\sigma}{dt}(Q^2, t) \Big|_{\text{SDG}}$. These coefficients correspond to a single emission.

3.2 The Exponent in the Conjugate Variable

Starting with the Borel representation (30) with the Borel function (31) we now calculate the exponent $\langle e^{-\nu t} \rangle_{\text{SDG}}$ as defined in (35),

$$\langle e^{-\nu t} \rangle_{\text{SDG}} = \frac{C_F}{\beta_0} \int_0^\infty dz B_\nu(z) \exp(-z \ln Q^2/\Lambda^2) \frac{\sin \pi z}{\pi z} \bar{A}_B(z) \quad (38)$$

with

$$B_\nu(z) \equiv \int_0^1 \frac{dt}{t} \left[\frac{2}{z} e^{2z \ln \frac{1}{t}} - \left(\frac{2}{z} + \frac{1}{1-z} + \frac{1}{2-z} \right) e^{z \ln \frac{1}{t}} \right] (e^{-\nu t} - 1). \quad (39)$$

To evaluate $B_\nu(z)$ we use the integral

$$\int_0^1 \frac{dt}{t} e^{z \ln \frac{1}{t}} (e^{-\nu t} - 1) = \nu^z \gamma(-z, \nu) + \frac{1}{z} \quad (40)$$

where

$$\gamma(-z, \nu) \equiv \Gamma(-z) - \Gamma(-z, \nu). \quad (41)$$

Note that (40) is regular at $z = 0$ due to cancellation between the γ function and the simple pole – the first originates in the $e^{-\nu t}$ part, i.e. in real contributions, while the latter in the unity, namely in virtual corrections. We thus find

$$B_\nu(z) = \frac{2}{z} \left[e^{2z \ln \nu} \gamma(-2z, \nu) + \frac{1}{2z} \right] - \left(\frac{2}{z} + \frac{1}{1-z} + \frac{1}{2-z} \right) \left[e^{z \ln \nu} \gamma(-z, \nu) + \frac{1}{z} \right]. \quad (42)$$

Similarly to (31), this Borel function is well defined at the perturbative level thanks to cancellation of the pole at $z = 0$ between the two terms in (42); the first corresponds to the large-angle soft gluon emission and the second to collinear gluon emission. In contrast[¶] with $B_{\text{SDG}}(z, t)$ in (31), $B_\nu(z)$ has a rich renormalon structure, making the integral (38) ambiguous at the level of power accuracy. Note that $\gamma(-z, \nu)$ has the same singularity structure as $\Gamma(-z)$: a simple pole at any non-negative integer. It follows that $B_\nu(z)$ in (42) has *two sets* of infrared renormalons: the first at all positive integers and half-integers due to large-angle emission sensitivity and the second at all positive integers – due to collinear sensitivity. In the latter, the renormalons at $z = 1$ and $z = 2$ become double poles. It is important to note that the $\sin(\pi z)$ factor in (38) regulates simple poles and transforms double poles into simple poles at all integer z values, while it does not affect the singularities at half integer z values. We will return to this point in the context of power-corrections in sec. 3.5.

An alternative representation of $\langle e^{-\nu t} \rangle_{\text{SDG}}$ in terms of a characteristic function can be obtained using eq. (29), namely

$$\begin{aligned} \langle e^{-\nu t} \rangle_{\text{SDG}} &= \frac{C_F}{\beta_0} \int_0^1 dt (e^{-\nu t} - 1) \int_{t^2}^t \frac{d\epsilon}{\epsilon} \bar{A}_{\text{eff}}(\epsilon Q^2) \left[-\frac{\epsilon^2}{t^3} - \frac{\epsilon}{t^2} + \frac{2}{t} \right] \\ &= \frac{C_F}{\beta_0} \int_0^1 \frac{d\epsilon}{\epsilon} \bar{A}_{\text{eff}}(\epsilon Q^2) \dot{\mathcal{F}}_\nu(\epsilon), \end{aligned} \quad (43)$$

[¶]At first sight it seems surprising that the Laplace-transformed $B_\nu(z)$ has a completely different renormalon structure from $B_{\text{SDG}}(z, t)$. The reason is, of course, that $B_\nu(z)$, thanks to the integration over t , is sensitive to the small t region, where the exponents $\exp(2zL)$ and $\exp(zL)$ in (31) are large and impose convergence constraints on (30).

where the order of integrations over t and ϵ has been changed. The characteristic function is given by,

$$\begin{aligned}\dot{\mathcal{F}}_\nu(\epsilon) &= \left(2 + \nu\epsilon - \frac{1}{2}\nu^2\epsilon^2\right) \text{Ei}(1, \sqrt{\epsilon}\nu) + \left(-\nu\epsilon - 2 + \frac{1}{2}\nu^2\epsilon^2\right) \text{Ei}(1, \nu\epsilon) \\ &+ \left(-\sqrt{\epsilon} - \frac{1}{2}\epsilon + \frac{1}{2}\nu\epsilon^{3/2}\right) e^{-\sqrt{\epsilon}\nu} + \left(\frac{3}{2} - \frac{1}{2}\nu\epsilon\right) e^{-\nu\epsilon} \\ &+ 2\ln(\sqrt{\epsilon}\nu) - 2\ln(\nu\epsilon) + \frac{1}{2}\epsilon + \sqrt{\epsilon} - \frac{3}{2}.\end{aligned}\quad (44)$$

Given a model* for the coupling which is regular in the infrared [22, 3], the integral (43) could be readily evaluated. We prefer, however, to complete the perturbative treatment without any additional assumptions on non-perturbative physics. For this purpose we find the Borel representation (42) most suitable: we shall define the perturbative sum as the principal value of the Borel integral (38). In the next section we calculate this integral explicitly, but before doing so it is worthwhile to examine more closely the structure of the sum, term by term.

Since we are interested in large ν we can replace $\gamma(-z, \nu)$ in (42) by $\Gamma(-z)$. The logarithmically enhanced terms are not modified by such a replacement. Expanding the integrand in (38) in powers of z , we obtain

$$\begin{aligned}B_\nu(z) &= \sum_{n=0}^{\infty} \frac{(\ln \nu)^n}{n!} \left[2 \sum_{m \geq \max\{1, n-1\}} (1 - 2^m) c_{m-n} z^{m-1} \right. \\ &\quad \left. + \sum_{l \geq 0} (1 + 2^{-l-1}) \sum_{m \geq \max\{n+l, n+1\}} c_{m-n-l-1} z^{m-1} \right],\end{aligned}\quad (45)$$

where the first term in the square brackets originates in the $2/t$ part in $\dot{\mathcal{F}}(\epsilon, t)$ from both the soft and collinear limits of phase-space, while the second originates in the ϵ dependent terms in $\dot{\mathcal{F}}(\epsilon, t)$ from the collinear limit alone. The numbers c_k are defined by $\Gamma(-z) = -\sum_{k=-1}^{\infty} c_k z^k$. This means that $c_{-1} = 1$, $c_0 = \gamma_E$, $c_1 = \pi^2/12 + \gamma_E^2/2$, etc. Higher c_k contain higher ζ_i numbers ($i \leq k+1$), yet numerically c_k ($k \geq 1$) are all close to 1.

Next, performing the Borel integral term by term we get a series in the coupling $\bar{A}(Q^2)$. It is then straightforward to rewrite the sum as

$$\left\langle e^{-\nu t} \right\rangle_{\text{SDG}} = \frac{C_F}{\beta_0} \sum_{k=1}^{\infty} \bar{A}(Q^2)^{k-2} \tilde{f}_k(\bar{A}(Q^2) \ln \nu) \quad (46)$$

and perform the summation over all powers of $\xi \equiv \bar{A}(Q^2) \ln \nu$. Writing

$$\tilde{f}_k(\xi) = \sum_{u=0}^{k/2} \left[(-\pi^2)^u / (2u+1)! \right] f_{k-2u}(\xi), \quad (47)$$

*An example is provided by [39].

the result for $k = 1$ and 2 is

$$\begin{aligned} f_1(\xi) &= 2(1 - \xi) \ln(1 - \xi) - (1 - 2\xi) \ln(1 - 2\xi) \\ f_2(\xi) &= -2\gamma_E (\ln(1 - \xi) - \ln(1 - 2\xi)) - \frac{3}{2} \ln(1 - \xi) \end{aligned} \quad (48)$$

and for $k \geq 3$,

$$\begin{aligned} f_k(\xi) &= (k-3)! \left\{ \left(2c_{k-2} + \sum_{m=0}^{k-2} (1 + 2^{-m-1}) c_{k-3-m} \right) \left[\left(\frac{1}{1-x} \right)^{k-2} - 1 \right] \right. \\ &\quad \left. - 2^{k-1} c_{k-2} \left[\left(\frac{1}{1-2x} \right)^{k-2} - 1 \right] \right\}, \end{aligned} \quad (49)$$

or, explicitly

$$\begin{aligned} f_3(\xi) &= -(\pi^2/6 + \gamma_E^2) \left[\frac{1}{(1-\xi)(1-2\xi)} - 1 \right] + (6\gamma_E + 5) \frac{\xi}{4(1-\xi)} \\ f_4(\xi) &= (4\zeta_3 + \pi^2\gamma_E + 2\gamma_E^3) \left[\frac{(4\xi-3)}{6(1-\xi)^2(1-2\xi)^2} + \frac{1}{2} \right] \\ &\quad + (\pi^2 + 6\gamma_E^2 + 10\gamma_E + 9) \frac{(2-\xi)\xi}{8(1-\xi)^2} \end{aligned} \quad (50)$$

etc. Here the function f_1 resums the leading-logs (LL), f_2 resums the next-to-leading logs (NLL) and so on. Note that if we ignore the effect of the analytic continuation to the time-like region the Borel integration simply gives $z^{m-1} \rightarrow (m-1)! \bar{A}^m$, which yields, upon resummation, the functions $f_k(\xi)$. Taking into account the analytic continuation amounts to $f_k(\xi) \rightarrow \tilde{f}_k(\xi)$. This has no effect on $f_1(\xi)$ and $f_2(\xi)$ and it has a minor effect on $f_k(\xi)$ for $k \geq 3$. We defined $f_k(\xi)$ such that they vanish at $\xi = 0$, thus excluding a constant coefficient. Such a constant does not necessarily exponentiate and it can be shifted into the “remainder function” $\ln R(y)|_{\text{non-log}}$ in (2).

The first two functions $f_1(\xi)$ and $f_2(\xi)$ are already known from [6]. When comparing $f_2(\xi)$ in (48) to [6] one should be careful concerning the definition of the coupling. Strictly speaking, our calculation is done in the large β_0 limit, so β_1 terms as well as other terms[†] which are sub-leading in β_0 are missing. However, these terms can be generated upon replacing the large β_0 coupling, which is one-loop, by a two-loop coupling in the “gluon bremsstrahlung” scheme [15] (see sec. 4) inside the integral (38). Such a replacement will be made in sec. 3.3 and then in the phenomenological analysis in sec. 5.

The functions $f_k(\xi)$, for $k \geq 2$ are singular at $\xi = 1/2$ and at $\xi = 1$; the first is associated with large-angle emission $\nu\bar{\Lambda}/Q \sim 1$ and the second with collinear emission $\nu\bar{\Lambda}^2/Q^2 \sim 1$. The singularity (at both limits) becomes stronger as the order k increases, in particular $f_k \sim 1/(1-2\xi)^{k-2}$ close to $\xi = 1/2$ and $f_k \sim 1/(1-\xi)^{k-2}$ close to $\xi = 1$, for any $k \geq 3$. Since soft gluon resummation has a universal structure, we expect that this singularity structure in ξ will be common to different physical processes. An example is

[†]Such terms originate [6] in the singular part of the NLO splitting function.

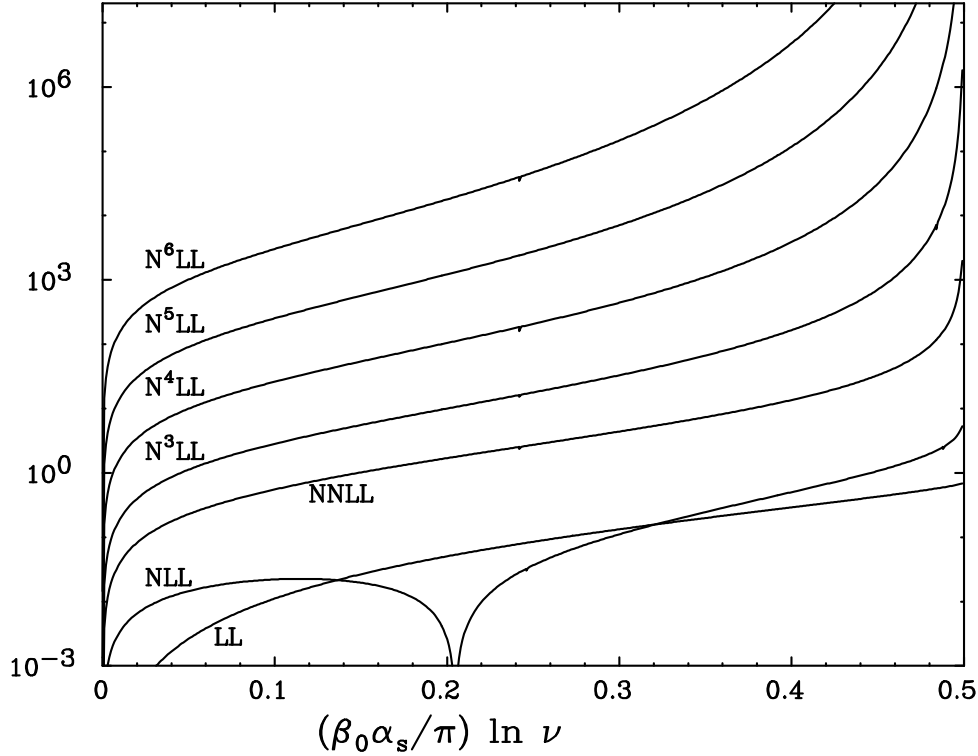


Figure 2: $\tilde{f}_k(\xi)$ for $k = 1$ (LL) through $k = 7$ (N^6 LL) as a function of $\xi \equiv \bar{A}(Q^2) \ln \nu$. The absolute value $|\tilde{f}_k(\xi)|$ is plotted on a logarithmic scale.

provided by a recent calculation of NNLL for deep-inelastic scattering and the Drell-Yan process [37]. There, the singularity structure of $f_k(\xi)$ for $k = 1$ through 3 is indeed similar to (48) and (50). In particular $f_3(\xi)$ has simple poles.

As usual in perturbation theory the expansion (46) is divergent. In principle it can be given sense e.g. by truncation at the minimal term. Note that this truncation is cumbersome since the minimal term will correspond to different orders depending on the value of ν . The standard procedure [6] amounts to truncating this expansion at NLL, so $\tilde{f}_k(\xi)$ for $k \geq 3$ are just neglected. To see whether this is legitimate let us now examine the numerical values of $\tilde{f}_k(\xi)$.

The functions $\tilde{f}_k(\xi)$ are plotted in fig. 2. It is clear from the plot that the expansion (46) is divergent. In particular, the ratios $\tilde{f}_k(\xi)/\tilde{f}_{k+1}(\xi)$ increase with k , reflecting factorial growth. The actual effect of these increasing coefficients depends on the value of the expansion parameter, here $\bar{A}(Q^2) = \beta_0 a(Q^2)$. $\bar{A}(Q^2)$ is defined in the “gluon bremsstrahlung” scheme [15] (the reason for this choice is explained in section 4). In fig. 3 we show the individual terms in (46) at two representative centre-of-mass energy scales: $Q = 91$ and 22 GeV. First note that the NNLL (\tilde{f}_3) gives a significant contribution in all cases. It should be emphasised that the leading part of its contribution is taken into account in the standard NLL calculation in the process of matching with the NLO result. Next note that N^3 LL (\tilde{f}_4) also gives quite an important correction: $\sim 8\%$

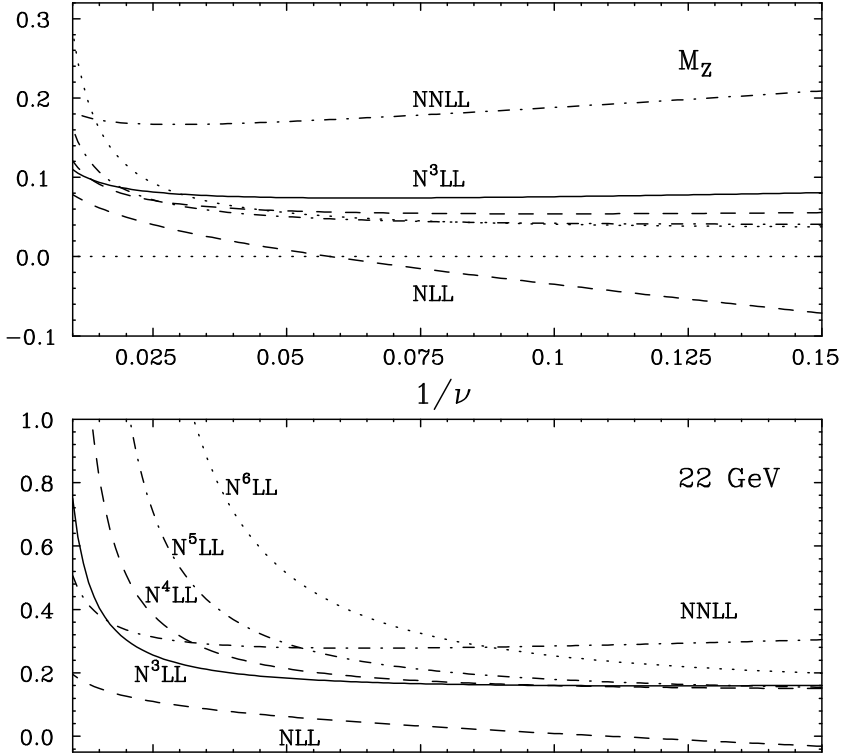


Figure 3: The relative significance of terms $\bar{A}(Q^2)^{k-2} \tilde{f}_k(\bar{A}(Q^2) \ln \nu)$ in (46) for $k = 2$ (NLL) through $k = 7$ (N^6LL) as a function of $1/\nu$ ($1/\nu \sim t$ in the small t region). In both plots, the terms are normalized by the LL function (1 on the vertical axis).

at M_Z and $\sim 20\%$ at 22 GeV . A closer examination shows that the hierarchy between the contributions of sub-leading logs depends strongly on both the energy (the value of the coupling) and $1/\nu$. At sufficiently large $1/\nu$ values, i.e. far enough from the two-jet limit, the expansion (46) appears to be convergent at the first few orders. Consider for example the case $1/\nu = 0.075$ at M_Z : the contribution of \tilde{f}_4 is smaller than that of \tilde{f}_3 and higher order terms continue decreasing up to \tilde{f}_6 . Then the trend changes: \tilde{f}_7 , which is the last line plotted, contributes slightly more than \tilde{f}_6 and the series starts diverging. In this particular example the contribution at the minimal term is about 4.4%. Thus a resummed perturbative calculation should not be expected to be better than that. For smaller $1/\nu$ values, and likewise at lower energies, the expansion diverges faster: the order at which the minimal term is reached becomes smaller while its contribution becomes larger. At some point, close to the distribution peak, the expansion becomes meaningless. Technically, this behaviour is a direct consequence of the enhanced singularity of the functions f_k and their factorially increasing numerical coefficients. This is the way infrared renormalons show up in this framework. Physically it is well expected that the perturbative expansion would gradually become less predictive and eventually irrelevant as a quantitative evaluation of the cross-section, since it misses non-perturbative soft gluon contributions or, in other words, hadronization effects. We shall return to this is-

sue in sec. 3.5. Until then, our goal is to complete the perturbative evaluation of the cross section. To achieve this we leave the expansion (46) and revert to Borel summation (38) which allows us, in rough terms, to resum the renormalons first, and then complete the summation over the logs.

3.3 Evaluation of the Borel sum

Our next task is to evaluate explicitly the Borel sum (38). An exact analytic integration is difficult. However, it is possible to make a systematic approximation of the Borel function and then perform the integration analytically.

We begin by writing the Borel function $B_\nu(z)$ as

$$B_\nu(z) = \frac{2}{z}V(2z) - \left(\frac{2}{z} + \frac{1}{1-z} + \frac{1}{2-z} \right) V(z) \quad (51)$$

with

$$V(z) \equiv e^{z \ln \nu} \Gamma(-z) + \frac{1}{z}. \quad (52)$$

Since $V(z)$ has only simple poles at positive integer z values, it is natural to approximate it by a rational function. Clearly, we would like the approximation to coincide with the function at least at the first few orders in the expansion around $z = 0$. One possibility is then to use Padé approximants based on some truncated sum. However, since we know the singularity structure, it is better to use an approximation of the form[‡]

$$V(z) \simeq \sum_{p=1}^{p_{\max}} \frac{r_p}{p - z}, \quad (53)$$

where r_p are set such that the expansion of this approximant coincides with that of (52) up to order $z^{p_{\max}-1}$. This means that r_p , for every $1 \leq p \leq p_{\max}$, is a polynomial of order p_{\max} in $\ln \nu$,

$$r_p = \sum_{q=0}^{p_{\max}} \rho_{p,q} (\ln \nu)^q \quad (54)$$

where $\rho_{p,q}$ are (irrational) numerical coefficients.

Next, $B_\nu(z)$ can be written as a sum of simple and double poles,

$$B_\nu(z) \simeq \sum_{n=1}^{p_{\max}} \frac{\bar{r}_{n/2}^{\text{la}}}{n/2 - z} + \sum_{p=1}^{p_{\max}} \frac{\bar{r}_p^{\text{col}}}{p - z} - \frac{r_1}{(1-z)^2} - \frac{r_2}{(2-z)^2} \quad (55)$$

where \bar{r}_p^{la} and \bar{r}_p^{col} are linear combinations of $\{r_p\}_{p=1}^{p_{\max}}$, corresponding to the large-angle (first term) and collinear (second term) parts of (51), respectively. Simple poles appear at all positive integers and half integers $1/2 \leq p \leq p_{\max}/2$ due to the large-angle part, and at all integers $3 \leq p \leq p_{\max}$ due to the collinear part. The double poles at $z = 1$

[‡]A similar approximation for the Borel function was used in [34] in a different application. Comparison with Padé approximants showed consistent results.

and $z = 2$ appear due to the collinear part. As an example, consider the case of $p_{\max} = 3$ where one has

$$B_\nu(z) \simeq \frac{2r_1}{\frac{1}{2} - z} + \frac{-3r_1 - \frac{1}{2}r_3}{1 - z} + \frac{\frac{2}{3}r_3}{\frac{3}{2} - z} + \frac{r_1 - r_3}{2 - z} + \frac{\frac{5}{6}r_3}{3 - z} - \frac{r_1}{(1 - z)^2} - \frac{r_2}{(2 - z)^2}.$$

Finally, given a specific coupling and the function (55) the Borel integral (38) can be evaluated analytically. The simple pole integrals are of the form

$$\begin{aligned} I_p(s) &= \int_0^\infty \exp(-z \ln Q^2/\Lambda^2) \frac{1}{p - z} \frac{\sin \pi z}{\pi z} \bar{A}_B(z) \\ &= \int_0^\infty \exp(-zs) \frac{1}{p - z} \frac{\sin \pi z}{\pi z} A_B(z) \end{aligned} \quad (56)$$

where $A_B(z)$ is the Borel transform of the $\overline{\text{MS}}$ coupling and $s \equiv \ln Q^2/\bar{\Lambda}^2$. Here Cauchy principal-value prescription is understood for $p > 0$. $I_p(s)$ can be written in terms of $\tilde{I}_p(s)$,

$$\tilde{I}_p(s) = \int_0^\infty \exp(-zs) \frac{1}{p - z} A_B(z), \quad (57)$$

by analytically continuing in s , $\bar{I}_p(s) = \frac{1}{2\pi i} (\tilde{I}_p(s - i\pi) - \tilde{I}_p(s + i\pi))$, and

$$I_p(s) = \frac{1}{p} \left[\bar{I}_p(s) - \lim_{p \rightarrow 0^-} \bar{I}_p(s) \right]. \quad (58)$$

The double pole integrals

$$I_p^{(1)}(s) = \int_0^\infty \exp(-zs) \frac{1}{(p - z)^2} \frac{\sin \pi z}{\pi z} A_B(z) \quad (59)$$

can be simply obtained using $I_p^{(1)}(s) = -\frac{d}{dp} I_p(s)$.

The simplest case is the one-loop running coupling, where $A_B(z) \equiv 1$. Here we have

$$\tilde{I}_p(s) \Big|_{\text{one-loop}} = -\text{Ei}(1, -ps) e^{-ps}. \quad (60)$$

The more difficult two-loop case was dealt with in [12] (see sec. 3.4 there) using results from [35]. It is useful to express the coupling using the Lambert W function [36],

$$\bar{A}(Q^2) \Big|_{\text{two-loop}} = -\frac{1}{\delta} \frac{1}{1 + w(s)} \quad (61)$$

where $\delta \equiv \beta_1/\beta_0^2$ and[§] $w(s) \equiv W_{-1}(-e^{-s/\delta-1})$. In these variables the two-loop renormalon integral (57) is simply

$$\tilde{I}_p(s) \Big|_{\text{two-loop}} = -[w(s)p\delta]^{p\delta} e^{w(s)p\delta} \Gamma(-p\delta, w(s)p\delta). \quad (62)$$

[§]The analytic continuation in the calculation of $\tilde{I}_p(s)$ should be done carefully: one should use the correct branch n of the Lambert W function, W_n . In practice this is simple since for $N_c = 3$, $N_f \leq 6$ the time-like axis is always contained in the $n = \pm 1$ branches (see [36] for more details).

In both (60) and (62) the principal value prescription amounts to taking the real part. Altogether the Borel integral (38) is given by

$$\langle e^{-\nu t} \rangle_{\text{SDG}} \simeq \frac{C_F}{\beta_0} \left[\sum_{n=1}^{p_{\max}} \bar{r}_{n/2}^{\text{la}} I_{n/2}(s) + \sum_{p=1}^{p_{\max}} \bar{r}_p^{\text{col}} I_p(s) - r_1 I_1^{(1)}(s) - r_2 I_2^{(1)}(s) \right], \quad (63)$$

where the (polynomial) dependence on $\ln \nu$ is fully contained in the coefficients \bar{r}_p and r_p , given by eqs. (52) through (54), while the dependence on the external energy scale $s \equiv \ln Q^2/\bar{\Lambda}^2$ is fully contained in the renormalon integrals $I_p(s)$. Eventually, the log-resummation order p_{\max} should be set large enough, so that higher orders can be safely neglected. In sec. 5 we show that in practice $p_{\max} \simeq 6$ is enough to make the result stable.

3.4 Evaluation of the inverse Laplace transform

The last stage of the calculation is to evaluate the inverse Laplace transform (37),

$$R(Q^2, t) \Big|_{\text{res}} = \int_C \frac{d\nu}{2\pi i \nu} e^{\nu t} \exp \left\{ \mathcal{S}_{\text{PT}}(Q^2, \ln \nu) \right\} \quad (64)$$

with $\mathcal{S}_{\text{PT}}(Q^2, \ln \nu) \equiv \langle e^{-\nu t} \rangle_{\text{SDG}}$. We apply the same technique used in [6] (see section 5 there). However, at a difference with the latter, we must keep track of sub-leading logs so we refrain from making any approximation. Defining $u = \nu t$ and expanding $\mathcal{S}(Q^2, \ln \nu) = \mathcal{S}(Q^2, L + \ln u)$ (where $L = \ln \frac{1}{t}$) in powers of $\ln u$, one has

$$\begin{aligned} R(Q^2, t) \Big|_{\text{res}} &= \int_C \frac{du}{2\pi i u} \exp \left\{ u + \mathcal{S}(Q^2, L + \ln u) \right\} \\ &= e^{\mathcal{S}(Q^2, L)} \int_C \frac{du}{2\pi i u} \exp \left\{ u + d_1(Q^2, L) \ln u + \sum_{k=2}^{\infty} \frac{1}{k!} d_k(Q^2, L) (\ln u)^k \right\} \end{aligned} \quad (65)$$

where $d_k(Q^2, L) \equiv \frac{d^k}{dL^k} \mathcal{S}(Q^2, L)$. Finally, we calculate $R(Q^2, t) \Big|_{\text{res}}$ by expanding

$$\exp \left\{ \sum_{k=2}^{\infty} \frac{1}{k!} d_k(Q^2, L) (\ln u)^k \right\}$$

in powers of $\ln u$ and using the integral

$$\int_C \frac{du}{2\pi i u} (\ln u)^n \exp \{u + g \ln u\} = \frac{d^n}{dg^n} \frac{1}{\Gamma(1-g)}. \quad (66)$$

Our final expression for $R(Q^2, t) \Big|_{\text{res}}$ includes several special functions: derivatives of the Γ function from (66) and the expressions for $I_p(\ln Q^2/\bar{\Lambda}^2)$, written in terms of the exponential integral function in the one-loop case (60), or the incomplete Γ function and the Lambert W function in the two-loop case (62). We therefore chose to evaluate it using the computer algebra program Maple.

3.5 Power-Corrections

Since hadronization is not described by perturbation theory it is a priori clear that there are non-perturbative corrections to the resummed cross-section. In this section we study the structure of these corrections. We already saw that the perturbative sum is, in general, ambiguous due to infrared renormalons. Having used a specific regularization of the renormalon singularities we are bound to address the question of the related power-suppressed ambiguity. The appearance of infrared renormalons does not only signal the existence of non-perturbative power-corrections, but also suggests their functional dependence on the energy and the event-shape variable. One should not expect, of course, that the entire non-perturbative contribution would be deducible from a perturbative result. Appropriate non-perturbative parameters will be introduced and eventually fixed by the data. Upon including these non-perturbative corrections the result becomes well-defined to power accuracy.

If the Borel sum (38) is supplemented by a non-perturbative contribution, eq. (64) becomes

$$R(Q^2, t) = \int_C \frac{d\nu}{2\pi i \nu} e^{\nu t} \exp \left\{ \mathcal{S}_{\text{PT}}(Q^2, \ln \nu) \right\} \exp \left\{ \mathcal{S}_{\text{NP}}(Q^2, \ln \nu) \right\}. \quad (67)$$

In sec. 3.4 we evaluated the inverse Laplace integral ignoring the non-perturbative part. Thanks to the factorized form of (67) non-perturbative corrections can be included by convoluting [2, 23, 24, 25] the perturbative result (64) with a non-perturbative function:

$$R(Q^2, t) = \int_0^t d\tilde{t} R(Q^2, t - \tilde{t}) \Big|_{\text{res}} f_{\text{NP}}(Q^2, \tilde{t}) \equiv R(Q^2, t) \Big|_{\text{res}} \star f_{\text{NP}}(Q^2, t) \quad (68)$$

where

$$f_{\text{NP}}(Q^2, t) = \int_C \frac{d\nu}{2\pi i} e^{\nu t} \exp \left\{ \mathcal{S}_{\text{NP}}(Q^2, \ln \nu) \right\}. \quad (69)$$

In order to learn about the functional form of $\mathcal{S}_{\text{NP}}(Q^2, \ln \nu)$, we shall now examine the renormalon structure of $\mathcal{S}_{\text{PT}}(Q^2, \ln \nu)$. Considering the integrand of (38) with $B_\nu(z)$ of eq. (42) (see description following the equation), we identify potential singularities at all positive integers and half integers. On the other hand, the $\sin \pi z$ factor which originates in the analytic continuation to the time-like region introduces an explicit zero at all integer z values. It is important to realize that the *complete* cancellation of some of the singularities may be an artifact of the large β_0 approximation. A similar situation occurs in any time-like observable, e.g. in the total cross-section [1]. There, having an operator product expansion, one can relate the singularity strength of the Borel[¶] pole $1/(p - z)^{1+\kappa}$ to the anomalous dimension of the corresponding operator(s) \mathcal{O}_p of dimension $2p$: $\kappa = p\beta_1/\beta_0^2 + \gamma_0/\beta_0$, where $[d/d\ln \mu^2 + \gamma] \mathcal{O}_p = 0$ with $\gamma = \gamma_0 (\alpha_s/\pi) + \dots$. Thus, in general, a large- β_0 calculation does not yield the correct singularity strength: not only the residue, but also κ is expected to be modified when sub-leading terms in β_0 are included. Being aware of this fact (and having no operator product expansion to

[¶]Note that the $p\beta_1/\beta_0^2$ term appears in the standard Borel transform but not in the scheme-invariant one [29, 30, 31].

supply additional information) it is reasonable to allow for modifications of order 1 in the singularities of $B_\nu(z)$,

$$b(z) = \frac{r_p}{(p-z)^m} \quad \longrightarrow \quad \tilde{b}(z) = \frac{\tilde{r}_p}{(p-z)^{m+\kappa_p}} \quad (70)$$

where we assume $|\kappa_p| < 1$. Thus, instead of simple and double poles ($m = 1, 2$), the Borel integrand has cuts which survive the suppression by the analytic continuation and introduce some ambiguity into $\mathcal{S}_{\text{PT}}(Q^2, \ln \nu)$. Note that we will not consider the possibility of a modified ν dependence of the exact Borel function compared to the calculated one. We allow only a modification of the overall coefficient and the singularity strength.

Consider first a scheme-invariant Borel integral in the space-like region,

$$\tilde{I}(s) = \int_0^\infty e^{-zs} \tilde{b}(z) dz, \quad (71)$$

where the Borel function behaves as (70) with $m = 1$ near $z = p$. The Borel integral can be written as a sum of two terms,

$$\begin{aligned} \tilde{I}(s) &= \int_0^p dz e^{-zs} \frac{1}{(p-z)^{1+\kappa}} + \int_p^\infty dz e^{-zs} \frac{1}{(p-z)^{1+\kappa}} \\ &= (-s)^\kappa \gamma(-\kappa, -sp) e^{-sp} - (-s)^\kappa \Gamma(-\kappa) e^{-sp} = -(-s)^\kappa \Gamma(-\kappa, -sp) e^{-sp}. \end{aligned}$$

Next we use the fact that the ambiguity $\Delta \tilde{I}(s)$ is purely imaginary and originates uniquely in the second integral where $z \geq p$, i.e. in the complete Γ function part^{||}. Taking $1/\pi$ times the imaginary part, we obtain

$$\Delta \tilde{I}(s) = -\frac{\sin(\pi\kappa)}{\pi} s^\kappa \Gamma(-\kappa) e^{-sp} = \frac{1}{\Gamma(1+\kappa)} s^\kappa e^{-sp}. \quad (72)$$

The ambiguity for the $m = 2$ case can be calculated using $\tilde{I}^{(1)}(s) = -\frac{d}{dp} \tilde{I}(s)$: one finds that $\Delta \tilde{I}^{(1)}(s) = \Delta \tilde{I}(s) s$. Substituting $s = \ln Q^2/\bar{\Lambda}^2$ we see that the ambiguity $\Delta \tilde{I}(s)$ scales as a power $(Q^2/\bar{\Lambda}^2)^p$, up to a logarithmic factor, $(\ln Q^2/\bar{\Lambda}^2)^\kappa$, which remains undetermined as long as κ is unknown. Next, the ambiguity of the corresponding Borel integral in the time-like region

$$I(s) = \int_0^\infty e^{-zs} \tilde{b}(z) \frac{\sin \pi z}{\pi z} dz, \quad (73)$$

can be deduced by analytically continuing (72) in $Q^2 \rightarrow -Q^2$, i.e. $s \rightarrow s \pm i\pi$, and taking $(\frac{1}{\pi p}$ times) the imaginary part,

$$\begin{aligned} \Delta I(s) &= \frac{1}{\pi p} \frac{(s^2 + \pi^2)^{\kappa/2}}{\Gamma(1+\kappa)} e^{-sp} \left[\cos\left(\kappa \arctan \frac{\pi}{s}\right) \sin(\pi p) - \sin\left(\kappa \arctan \frac{\pi}{s}\right) \cos(\pi p) \right] \\ &\simeq \frac{1}{\pi p} \frac{1}{\Gamma(1+\kappa)} s^\kappa e^{-sp} \left[\sin(\pi p) - \frac{\kappa \pi}{s} \cos(\pi p) \right], \end{aligned} \quad (74)$$

^{||}A similar mathematical analysis appears in [12] in the context of a renormalon integral with a two-loop running coupling.

where the expression in the second line is obtained expanding in $1/s$ and neglecting $1/s^2$ terms and higher. Similarly, we obtain

$$\Delta I^{(1)}(s) \simeq \frac{1}{\pi p} \frac{1}{\Gamma(1+\kappa)} s^\kappa e^{-sp} [s \sin(\pi p) - (1+\kappa)\pi \cos(\pi p)]. \quad (75)$$

Given the general singularity structure of the SDG Borel function $B_\nu(z)$ around $z = p$,

$$b(z) = \frac{r_p^{(1)}}{(p-z)^2} + \frac{r_p}{p-z}, \quad (76)$$

our result for the ambiguity ((74) and (75)) suggests the following assignments of non-perturbative contributions,

$$I_{\text{NP}}(s) = \frac{\rho_{2p}}{\pi p} \frac{e^{-sp} s^{\kappa_p}}{\Gamma(1+\kappa_p)} \left[(r_p^{(1)} s + r_p) \sin(\pi p) - ((1+\kappa_p) r_p^{(1)} + \kappa_p r_p/s) \pi \cos(\pi p) \right], \quad (77)$$

where $s = \ln Q^2/\bar{\Lambda}^2$ and ρ_{2p} are dimensionless phenomenological parameters to be fixed, eventually, by the data. On general grounds we expect that $\rho_{2p} \sim \mathcal{O}(1)$. It is important to keep in mind that the actual values of ρ_{2p} depend on the regularization prescription used for the Borel sum. For example, when the perturbative sum is defined using a cut-off (on the Euclidean momentum), ρ_{2p} can be interpreted as moments of an “infrared finite effective coupling” $\bar{A}_{\text{NP}}(k^2)$ [22, 12], which is assumed to coincide with the perturbative coupling $\bar{A}_{\text{PT}}(k^2)$ above some scale μ_I ($\bar{\Lambda} \ll \mu_I \ll Q$),

$$\rho_{2p}^{\mu_I} = \left(\frac{\mu_I^2}{\bar{\Lambda}^2} \right)^p m_p^{\text{NP}}(\mu_I^2) \quad (78)$$

where

$$m_p^{\text{NP}}(\mu_I^2) \equiv \int_0^{\mu_I^2} p \frac{dk^2}{k^2} \left(\frac{k^2}{\mu_I^2} \right)^p \bar{A}_{\text{NP}}(k^2). \quad (79)$$

When the perturbative sum is defined in terms of the principal value of the Borel integral, ρ_{2p} is

$$\rho_{2p}^{\text{PV}} = \left(\frac{\mu_I^2}{\bar{\Lambda}^2} \right)^p [m_p^{\text{NP}}(\mu_I^2) - m_p^{\text{PT}}(\mu_I^2)] \quad (80)$$

where

$$m_p^{\text{PT}}(\mu_I^2) \equiv \text{P.V.} \int_0^{\mu_I^2} p \frac{dk^2}{k^2} \left(\frac{k^2}{\mu_I^2} \right)^p \bar{A}_{\text{PT}}(k^2). \quad (81)$$

Note that ρ_{2p}^{PV} are independent of μ_I . A detailed comparison of the two regularization prescriptions can be found in [12]. The explicit expressions for $m_p^{\text{PT}}(\mu_I^2)$ in the one-loop and two-loop cases can be obtained by substituting $s \rightarrow \ln \mu_I^2/\bar{\Lambda}^2$ in eqs. (60) and (62) (taking the real part and multiplying by p), respectively.

Let us now examine in more detail the singularities in (42). First note that double poles at half integer values do not occur. Thus the term $r_p^{(1)} s \sin(\pi p)$ in (77) is actually not relevant. Next, to determine the residues r_p of $B_\nu(z)$ we use the fact that**

**Since our interest is in large ν values, corresponding to small t , we can replace $\gamma(-z, \nu)$ by $\Gamma(-z)$, which is a good approximation at any $\nu > 1$.

Residue $\{\Gamma(-z)\} = (-1)^{p+1}/p!$, and therefore Residue $\{\Gamma(-2z)\} = (-1)^{2p+1}/(2(2p)!)$. Consider the first term in (42) which is related to large-angle emission. Here $r_p^{la} = \frac{1}{p(2p)!} \nu^{2p} (-1)^{2p}$ and there are no double poles, so

$$I_p^{la} = \frac{-\rho_{2p}}{\pi p^2 (2p)! \Gamma(1 + \kappa_p)} \left(\frac{\nu \bar{\Lambda}}{Q} \right)^{2p} \left[\left(\ln \frac{Q^2}{\bar{\Lambda}^2} \right)^{\kappa_p} \sin(\pi p) + \kappa_p \pi \left(\ln \frac{Q^2}{\bar{\Lambda}^2} \right)^{\kappa_p-1} \cos(\pi p) \right]. \quad (82)$$

Summing over p this gives

$$\left\langle e^{-\nu t} \right\rangle_{NP}^{\text{large-angle}} = - \sum_{p=\frac{1}{2}, 1, \frac{3}{2}, 2, \frac{5}{2}, \dots} \lambda_{2p} \frac{1}{(2p)!} \left(\frac{\nu \bar{\Lambda}}{Q} \right)^{2p} = - \sum_{n=1}^{\infty} \lambda_n \frac{1}{n!} \left(\frac{\nu \bar{\Lambda}}{Q} \right)^n \quad (83)$$

where we defined

$$\begin{aligned} 2p \text{ odd} \quad \lambda_{2p} &= \frac{C_F}{\beta_0} \frac{\rho_{2p}}{p^2} \frac{1}{\Gamma(1 + \kappa_p)} \left(\ln Q^2 / \bar{\Lambda}^2 \right)^{\kappa_p} \frac{\sin(\pi p)}{\pi} \\ 2p \text{ even} \quad \lambda_{2p} &= \frac{C_F}{\beta_0} \frac{\rho_{2p}}{p^2} \kappa_p \frac{1}{\Gamma(1 + \kappa_p)} \left(\ln Q^2 / \bar{\Lambda}^2 \right)^{\kappa_p-1} \cos(\pi p). \end{aligned} \quad (84)$$

The second term in (42), associated with collinear emission, is treated in a similar manner. Note that here there are also double poles at $p = 1$ and 2 and consequently the residues have a more complicated dependence on ν . The result is

$$\begin{aligned} \left\langle e^{-\nu t} \right\rangle_{NP}^{\text{col}} &= -\lambda_2^{(1)} \frac{\nu \bar{\Lambda}^2}{Q^2} - \lambda_4^{(1)} \frac{\nu^2 \bar{\Lambda}^4}{Q^4} \\ &- [(4 - \gamma_E - \ln \nu) \nu - 1] \lambda_2 \frac{\bar{\Lambda}^2}{Q^2} - \left[\left(-\frac{3}{2} + \gamma_E + \ln \nu \right) \nu^2 - 1 \right] \lambda_4 \frac{\bar{\Lambda}^4}{Q^4} \\ &- \sum_{p \geq 3}^{\infty} \lambda_{2p} \left(\frac{2}{p} + \frac{1}{1-p} + \frac{1}{2-p} \right) \frac{(-1)^{p+1}}{(p-1)!} \left(\frac{\nu \bar{\Lambda}^2}{Q^2} \right)^p, \end{aligned} \quad (85)$$

where the first line corresponds to the double poles at $p = 1$ and 2 , with

$$\lambda_{2p}^{(1)} = -\frac{C_F}{\beta_0} \frac{\rho_{2p}}{p} \frac{(1 + \kappa_p)}{\Gamma(1 + \kappa_p)} \left(\ln Q^2 / \bar{\Lambda}^2 \right)^{\kappa_p};$$

the second line corresponds to the simple poles at $p = 1$ and 2 , and the last line to the remaining simple poles at integers $p \geq 3$. λ_{2p} are given in (84).

Finally, the total non-perturbative contribution in (67) is given by

$$\mathcal{S}_{NP}(Q^2, \ln \nu) \equiv \left\langle e^{-\nu t} \right\rangle_{NP}^{\text{large-angle}} + \left\langle e^{-\nu t} \right\rangle_{NP}^{\text{col}}. \quad (86)$$

Note that in both (83) and (85) we use the same non-perturbative parameters ρ_{2p} . One could introduce a more general parametrisation of power-corrections by defining separate parameters for the large-angle and collinear regions of phase-space. This, however, seems

redundant from the current point of view: compensating the ambiguity in the perturbative sum does not require separate parameters. Moreover, the delicate relation between the large-angle and collinear limits of phase-space at the perturbative level suggests that the two are correlated in the same way also at the non-perturbative level.

It is now straightforward to see the relation with previously suggested models for power-corrections [2, 23, 3, 24, 25, 26]. As mentioned in the introduction, it was shown [2, 23, 3] that the primary non-perturbative effect in the region $t \gg \bar{\Lambda}/Q$ is a shift of the resummed distribution to larger values of t :

$$\frac{1}{\sigma} \frac{d\sigma}{dt} \bigg|_{\text{res}} (Q^2, t) \longrightarrow \frac{1}{\sigma} \frac{d\sigma}{dt} \bigg|_{\text{res}} (t - \lambda_1 \bar{\Lambda}/Q). \quad (87)$$

This is indeed the effect if one keeps only the first term in the sum in (83): then the only non-perturbative contribution to $\mathcal{S}_{\text{NP}}(Q^2, \ln \nu)$ in (67) is $\lambda_1 \nu \bar{\Lambda}/Q$, and

$$f_{\text{la}} = \delta(t - \lambda_1 \bar{\Lambda}/Q). \quad (88)$$

Assuming that the average thrust is dominated by the two-jet region, the corresponding correction is $\langle t \rangle \longrightarrow \langle t \rangle + \lambda_1 \bar{\Lambda}/Q$, namely it is the same parameter that controls the shift of the distribution and the leading power-correction to $\langle t \rangle$. This $1/Q$ correction to the average thrust was discussed extensively in the literature [19, 20, 21, 22, 32, 25, 12, 27].

As explained in [25, 26], the shift (87) is no longer adequate when $t \simeq \bar{\Lambda}/Q$. The shape-function [2, 23, 24, 25, 26] allows parametrisation of all the terms in (83) making the following identification:

$$\int_0^\infty d\tilde{t} \exp(-\nu \tilde{t}) (Q/\bar{\Lambda}) f_{\text{la}}(\tilde{t}Q/\bar{\Lambda}) = \exp \left\{ \left\langle e^{-\nu t} \right\rangle_{\text{NP}}^{\text{large-angle}} \right\}. \quad (89)$$

The single argument function $(Q/\bar{\Lambda}) f_{\text{la}}(tQ/\bar{\Lambda})$ is therefore a particular example of the two-argument non-perturbative function $f_{\text{NP}}(Q^2, t)$ defined in eqs. (68) and (69). Similarly to [25, 26], the moments of the large-angle shape-function $\sigma_m \equiv \int_0^\infty f_{\text{la}}(\epsilon) \epsilon^m d\epsilon$ are related to the parameters λ_{2p} . Writing (89) as

$$\int_0^\infty \exp \left\{ -\frac{\nu \epsilon \bar{\Lambda}}{Q} \right\} f_{\text{la}}(\epsilon) d\epsilon = \exp \left\{ - \sum_{n=1}^{\infty} \lambda_n \frac{1}{n!} \left(\frac{\nu \bar{\Lambda}}{Q} \right)^n \right\} \quad (90)$$

and expanding the exponents on both sides one has:

$$\sigma_0 = 1, \quad \sigma_1 = \lambda_1, \quad \sigma_2 = \lambda_1^2 - \lambda_2, \quad \sigma_3 = \lambda_1^3 - 3\lambda_1\lambda_2 + \lambda_3. \quad (91)$$

The function $f_{\text{la}}(\epsilon)$, like the parameters λ_{2p} , depends on the regularization prescription of the perturbative calculation. In the absence of a non-perturbative calculation (ref. [25] gives a field theoretic definition) the shape-function and thus λ_n can only be determined by fitting the data.

Finally, to deal with the collinear power-corrections, one should include (85). Here, the most important corrections arise from the terms that are enhanced by $\ln \nu$. Note that the *remaining* terms can be simply recast in the form

$$\int_0^\infty d\tilde{t} \exp(-\nu \tilde{t}) (Q^2/\bar{\Lambda}^2) f_{\text{col}}^{\text{sub-leading}}(\tilde{t}Q^2/\bar{\Lambda}^2) \quad (92)$$

similarly to the shape-function of (89). These corrections become important only at $t \sim \bar{\Lambda}^2/Q^2$ and can be safely neglected in the region $t \simeq \bar{\Lambda}/Q$. To treat the terms that are enhanced by $\ln \nu$ we first expand the exponent,

$$\begin{aligned} \exp \left\{ \left\langle e^{-\nu t} \right\rangle_{\text{NP}}^{\text{col}} \right\} &= 1 + \lambda_2 \frac{\nu \bar{\Lambda}^2}{Q^2} (\ln \nu + \gamma_E) + \left[\frac{\lambda_2^2}{2} (\ln \nu + \gamma_E)^2 - \lambda_4 (\ln \nu + \gamma_E) \right] \frac{\nu^2 \bar{\Lambda}^4}{Q^4} \\ &+ \left[\frac{\lambda_2^3}{6} (\ln \nu + \gamma_E)^3 - \lambda_2^2 \lambda_4 (\ln \nu + \gamma_E)^2 \right] \frac{\nu^3 \bar{\Lambda}^6}{Q^6} + \dots, \end{aligned} \quad (93)$$

where we kept the sub-leading γ_E constants for convenience (see below). Next we use the fact that

$$\Gamma(\epsilon) \nu^{-\epsilon} = \int_0^\infty dt \frac{1}{t} t^\epsilon e^{-\nu t}$$

to write the following convolution integral in the “+” prescription, with a generic test function $h(t)$ whose inverse Laplace transform is $H(\nu)$,

$$\begin{aligned} \left[\Gamma(\epsilon) \nu^{-\epsilon} - \frac{1}{\epsilon} \right] H(\nu) &= \int_0^\infty dt e^{-\nu t} \int_0^t d\tilde{t} \left[\frac{1}{\tilde{t}} e^{\epsilon \ln \tilde{t}} \right]_+ h(t - \tilde{t}) \\ &= \int_0^\infty dt e^{-\nu t} \int_0^t d\tilde{t} \frac{1}{\tilde{t}} e^{\epsilon \ln \tilde{t}} [h(t - \tilde{t}) - h(t)] \end{aligned} \quad (94)$$

Now one can extract the inverse Laplace transform of the terms in (93), in the distribution sense, by expanding both sides of eq. (94) in powers of ϵ . In particular, one has

$$\int_0^\infty dt \left[\frac{1}{t} \right]_+ e^{-\nu t} = -(\ln \nu + \gamma_E) \quad \int_0^\infty dt \left[\frac{\ln t}{t} \right]_+ e^{-\nu t} = \frac{1}{2} (\ln \nu + \gamma_E)^2 + \frac{\pi^2}{12}.$$

Thus,

$$\begin{aligned} f_{\text{col}}(Q^2, t) &= \int_C \frac{d\nu}{2\pi i} e^{\nu t} \exp \left\{ \left\langle e^{-\nu t} \right\rangle_{\text{NP}}^{\text{col}} \right\} \\ &= \delta(t) - \lambda_2 \left[\frac{\bar{\Lambda}^2}{Q^2 t} \right]_+ \star \delta^{(1)}(t) + \left[\lambda_2^2 \frac{\bar{\Lambda}^4}{Q^4} \left(\frac{\ln t}{t} - \frac{\pi^2}{12} \delta(t) \right) + \lambda_4 \frac{\bar{\Lambda}^4}{Q^4 t} \right]_+ \star \delta^{(2)}(t) + \dots \\ &= \left[1 + \lambda_2 \frac{\bar{\Lambda}^2}{Q^2 t^2} - \left(2\lambda_2^2 \ln \frac{1}{t} + \mathcal{O}(1) \right) \frac{\bar{\Lambda}^4}{Q^4 t^3} + \mathcal{O} \left(\frac{\bar{\Lambda}^6}{Q^6 t^4} \right) \right] \delta(t), \end{aligned} \quad (95)$$

where $\delta^{(n)}(t)$ is the n -th derivative of the δ -function^{††}. Clearly, the leading correction $\frac{\lambda_2^2}{Q^2 t^2}$ is as important around $t \simeq \bar{\Lambda}/Q$ as the large-angle corrections contained in the shape-function (89). The sub-leading terms in (95) are less important and can be ignored in a first approximation.

In conclusion, the most important power correction at $t \gg \bar{\Lambda}/Q$ is the one associated with the simple renormalon pole at $z = \frac{1}{2}$. Its exponentiation amounts to a shift of the resummed distribution by $\lambda_1 \bar{\Lambda}/Q$. Closer to the two-jet region sub-leading power corrections of the form $\lambda_n (\bar{\Lambda}/tQ)^n$ become important. Strictly based on the large β_0

^{††}In the last line, the appropriate integration prescription at $t \rightarrow 0$ is understood.

renormalon calculation, only odd values associated with renormalon poles at half integers, are relevant. However, since the large β_0 limit is not expected to predict the singularity strength of the exact Borel transform, one should expect $\lambda_n(\bar{\Lambda}/tQ)^n$ with even n to survive. Assuming that the exact Borel function differs from the calculated one only by a modification of the singularity strength, with the ν dependence left unchanged, we predict that the even terms will be suppressed by $1/\ln(Q^2/\bar{\Lambda}^2)$ compared to the odd ones (see 84). Allowing both odd and even terms in the sum in (90) one recovers the shape-function description as far as the large-angle gluon emission is concerned. Nevertheless, at the same time a collinear correction proportional to $\lambda_2(\bar{\Lambda}/tQ)^2$ appears in (95). The latter has a sign apposite to the relevant term in the large-angle shape-function, with a slightly different functional form, thus reducing significantly the overall effect of the non-perturbative parameter λ_2 .

Finally, we comment that an alternative way to derive the form of the power corrections from the large β_0 calculation is to use the characteristic function (44). Expanding the latter at small ϵ one obtains

$$\begin{aligned}\dot{\mathcal{F}}_\nu(\epsilon) &= 2\sqrt{\epsilon}\nu + \left(-\frac{1}{2}\nu\ln\left(\frac{1}{\epsilon}\right) - 3\nu - \frac{1}{2}\nu^2\right)\epsilon + \left(\nu + \frac{1}{2}\nu^2 + \frac{1}{9}\nu^3\right)\epsilon^{3/2} \\ &+ \left(\frac{1}{4}\nu^2\ln\left(\frac{1}{\epsilon}\right) - \frac{1}{12}\nu^3 - \frac{1}{48}\nu^4\right)\epsilon^2 + \left(-\frac{1}{6}\nu^3 + \frac{1}{72}\nu^4 + \frac{1}{300}\nu^5\right)\epsilon^{5/2} \\ &+ \left(\frac{5}{36}\nu^3 + \frac{1}{48}\nu^4 - \frac{1}{480}\nu^5 - \frac{1}{2160}\nu^6\right)\epsilon^3 \\ &+ \left(-\frac{1}{360}\nu^5 + \frac{1}{3600}\nu^6 + \frac{1}{17640}\nu^7\right)\epsilon^{7/2} + \dots\end{aligned}$$

Here only non-analytic terms are associated with ambiguity of the perturbative sum (43), and therefore with power corrections [22, 1]. One can immediately identify the terms $(\nu\sqrt{\epsilon})^n$ where $n = 1, 3, 5, \dots$ as the half-integer renormalon poles associated with large-angle soft gluons. These are the most important power corrections. As for integer powers ϵ^p , the only non-analytic terms are at $p = 1$ and $p = 2$, due to the logarithm. These ambiguities, however, are negligible for any $t \gg \bar{\Lambda}^2/Q^2$ since each power of ϵ is accompanied by ν rather than by ν^2 . Thus the picture is consistent with what we already learned based on the Borel analysis in the case that the singularities at integer z are just simple poles and are therefore cancelled by $\sin(\pi z)$ factor from the analytic continuation.

4 Thrust Distribution from the Splitting Function

The standard way of calculating the logarithmically enhanced cross-section [6] is based on an evolution equation for the jet mass distribution $J(Q^2, k^2)$, where the kernel is the splitting function of a gluon off a quark, $P(a, x)$. At leading order the splitting function is

$$P(a, x) = C_F a \left[\frac{x}{1-x} + \frac{1}{2}(1-x) \right]_+ = C_F a \left[\frac{1}{1-x} - \frac{1}{2}(1+x) \right]_+ \quad (96)$$

where $a(k^2)$ is the coupling $(\alpha_s(k^2)/\pi)$ and x is the longitudinal momentum fraction in the branching. Fixing the coupling to be the “gluon bremsstrahlung” coupling [15],

$$a \longrightarrow \tilde{a} \equiv a_{\overline{\text{MS}}} + \left[\frac{5}{3} \beta_0 + \left(1 - \frac{\pi^2}{12} \right) C_A \right] a_{\overline{\text{MS}}}^2 + \dots \quad (97)$$

this splitting function is correct to next-to-leading order, as far as the singular $1/(1-x)$ terms are concerned. At NLL accuracy, the evolution equation is [6],

$$\frac{dJ_\nu(Q^2)}{d \ln Q^2} = \int_0^1 dx P(\tilde{a}((1-x)Q^2), x) [e^{-\nu(1-x)} - 1] J_\nu(Q^2) \quad (98)$$

where $J_\nu(Q^2)$ is the Laplace transform of $J(Q^2, k^2)$ with respect to k^2/Q^2 . The solution of this differential equation is [6]

$$\ln J_\nu(Q^2) = \int_0^1 [e^{-\nu u} - 1] \frac{1}{u} \int_0^{1-u} dx P(\tilde{a}((1-x)uQ^2), x). \quad (99)$$

To this accuracy 1— thrust, t , is the sum of invariant masses of the two hemispheres, so

$$R(Q^2, t) = \int_0^\infty dk^2 d\bar{k}^2 J(Q^2, k^2) J(Q^2, \bar{k}^2) \theta(tQ^2 - k^2 - \bar{k}^2), \quad (100)$$

and therefore,

$$R(Q^2, t) \Big|_{\text{res}} = \int_C \frac{d\nu}{2\pi i \nu} e^{\nu t} \exp\{2 \ln J_\nu(Q^2)\}. \quad (101)$$

From here, a straightforward calculation gives the leading and next-to-leading logs in the thrust distribution.

Let us now compare this calculation with ours. Specifically, $2 \ln J_\nu(Q^2)$ in (101) should be compared with $\langle e^{-\nu t} \rangle_{\text{SDG}}$ in (36). The two quantities are defined in (99) and (35), respectively. The first observation is that the integration variable u in (99) can be identified with t , making the two similar provided one identifies

$$\frac{1}{\sigma} \frac{d\sigma}{dt}(Q^2, t) \Big|_{\text{SDG}} \longleftrightarrow \frac{2}{t} \int_0^{1-t} dx P(\tilde{a}((1-x)tQ^2), x), \quad (102)$$

or, explicitly (see 29),

$$\int_{t^2}^t \frac{d\epsilon}{\epsilon} \bar{A}_{\text{eff}}(\epsilon Q^2) \left[\frac{2}{t} - \frac{\epsilon}{t^2} - \frac{\epsilon^2}{t^3} \right] \longleftrightarrow \frac{2}{t} \int_0^{1-t} dx \beta_0 \tilde{a}((1-x)tQ^2) \left[\frac{1}{1-x} - \frac{1}{2}(1+x) \right]. \quad (103)$$

If one identifies $\bar{A}_{\text{eff}}(\epsilon Q^2)$ with $\beta_0 \tilde{a}((1-x)tQ^2)$, and changes variables $\epsilon = (1-x)t$, the r.h.s. becomes

$$\int_{t^2}^t \frac{d\epsilon}{\epsilon} \bar{A}_{\text{eff}}(\epsilon Q^2) \left[\frac{2}{t} - \frac{2\epsilon}{t^2} + \frac{\epsilon^2}{t^3} \right].$$

One thus finds that the first term in the square brackets on both sides is the same. Recall that this term is responsible for the leading logs. The other terms, contributing to sub-leading logs, are not the same. However, the NLL are: to NLL accuracy it is enough to

consider the conformal part [6] by fixing the scale of the coupling. The latter gives, in both cases, $-\frac{1}{t} \frac{3}{2} \bar{A}(Q^2)$ from the collinear limit $\epsilon = t$.

We thus learned that DGE is consistent with the exact exponent to NLL accuracy provided one identifies the running coupling with the “gluon bremsstrahlung” coupling [15] of eq. (97). In evaluating the Borel sum (38) we therefore use

$$\bar{A}(k^2) = \frac{A(k^2)}{1 - \left[\frac{5}{3} + \left(1 - \frac{\pi^2}{12}\right) C_A / \beta_0 \right] A(k^2)}. \quad (104)$$

instead of (6). This simply amounts to fixing the definition of $\bar{\Lambda}$ (see (27)).

The qualitative features of the SDG characteristic-function based calculation appear also in the splitting-function based calculation: there appear ϵ/t^2 and ϵ^2/t^3 terms which contribute to the log-enhanced cross-section due to the collinear limit $\epsilon \simeq t$. As we saw in the previous sections these terms lead to factorial enhancement of sub-leading logs (already prior to exponentiation). However, the actual values of sub-leading logs predicted by the splitting-function beyond the NLL are different. Performing the integral on the r.h.s. of (103) explicitly we arrive at the following expansion for $\frac{1}{\sigma} \frac{d\sigma}{dt}(Q^2, t)$ prior to exponentiation:

$$\begin{aligned} \frac{1}{\sigma} \frac{d\sigma}{dt}(Q^2, t) &= \frac{C_F}{t \beta_0} \left\{ (2. L - 1.5) A(Q^2) + (3 L^2 + 1.8333 L - 4.2500) A(Q^2)^2 \right. \quad (105) \\ &+ (4.6667 L^3 + 8.5000 L^2 - 9.5242 L - 8.8151) A(Q^2)^3 \\ &+ (7.5000 L^4 + 21.833 L^3 - 17.359 L^2 - 50.085 L - 9.957) A(Q^2)^4 \\ &+ (12.400 L^5 + 48.500 L^4 - 31.339 L^3 - 194.72 L^2 - 95.096 L + 10.97) A(Q^2)^5 + \dots \end{aligned}$$

This expansion can be compared directly with (29). The LL and NLL are of course the same. Sub-leading logs are similar in many cases; note in particular the NNLL. Nevertheless, at lower logs there are big variations, as one can deduced directly from (103).

The fact that the two calculations differ beyond NLL is of no surprise. Most importantly, the kinematic approximations made in the splitting-function based calculation (e.g. the matrix element, the definition of the observable), modify the logs beyond NLL accuracy.

It should be emphasised that some approximations have been made also in the characteristic-function based calculation. Although this calculation is *exact* at the level of three partons with an off-shell gluon, there are approximations beyond this level: the massive-gluon characteristic-function does not take into account the possible branching of the gluon into opposite hemispheres, the so-called non-inclusive contribution. When the gluon is roughly collinear with one of the quarks (the only limit contributing to sub-leading logs in $\frac{1}{\sigma} \frac{d\sigma}{dt}(Q^2, t) \Big|_{\text{SDG}}$) this type of branching is probably not significant. Indeed, the comparison between $\frac{1}{\sigma} \frac{d\sigma}{dt}(Q^2, t) \Big|_{\text{SDG}}$ and the leading term in β_0 in the (numerically evaluated) exact NLO coefficient in sec. 2.2 confirms this assertion. Another important aspect is the validity of the exponentiation formula (37) beyond NLL accuracy. As discussed in sec. 3, correlations in the emission of multiple soft and collinear gluons may influence the sub-leading logs. This effect was neglected.

5 The phenomenological implication

We saw that a careful treatment of running coupling effects (or renormalons) in the logarithmically enhanced cross-section requires resummation of sub-leading logs. Our investigation in section 3.2 leaves no doubt: sub-leading logs contribute significantly at all physically interesting values of the thrust. On the other hand, it is well known that successful fits to the distribution were obtained in [3, 26, 25] with a much simpler treatment of the perturbative calculation, based on the standard NLL resummation. Non-perturbative corrections whose magnitude is not under control theoretically are anyway important, and must be included in any fit. One may argue that a more complete perturbative treatment is not necessary, and that it amounts simply to a redefinition of the non-perturbative correction. The answer is, of course, that as soon as quantitative predictions are expected one should start with a reliable perturbative calculation. Physically, the transition between the perturbative and non-perturbative regimes is smooth, and one must make sure that an arbitrary separation of the two does not have too strong an impact on the results. Legitimate separations are cut-off regularization of momentum integrals and principal-value Borel summation. It was shown in [12] that these two procedures can be fully consistent with each other provided that renormalon resummation is performed. This means in particular that the extracted value of α_s is the same using the two prescriptions. Such consistency cannot be achieved if a truncated perturbative expansion, e.g. NLO, is used instead. Our results in sec. 3.2 imply that NLL truncation of the exponent is just as dangerous. By performing renormalon resummation, such a truncation is avoided and a more reliable comparison with data can be achieved.

Here we shall perform global fits to the thrust distribution at all energies, based on our perturbative calculation of section 3. As discussed in section 3.3 we use principal-value Borel summation. An equivalent calculation can be done using cut-off regularization. The translation of our results to this language is straightforward and may be useful once comparison can be made to a non-perturbative calculation of the shape-function with a hard cut-off as an ultraviolet regulator.

The perturbative calculation must be supplemented by non-perturbative corrections in order to be compared with the data. Our guiding principle is that the functional form of the non-perturbative corrections is dominated by the ambiguities identified in the calculation of the perturbative sum. We assume that the SDG based calculation is sufficient to identify these ambiguities. Of course, there are inherent limitations to this calculation: splitting of a gluon into partons that end up in opposite hemispheres is not taken into account, nor are correlations between the emitted gluons. These effects are not expected to be important in the two-jet region, so it is reasonable to neglect them.

5.1 Perturbative calculation

Before attempting any fits to the data involving non-perturbative corrections, it is useful to examine the impact of the resummation simply by looking at the perturbatively calculated cross-section in fig. 4. Needless to say, the fixed-order calculations, LO and NLO, do not describe the physical cross section in the two-jet region. The large differ-

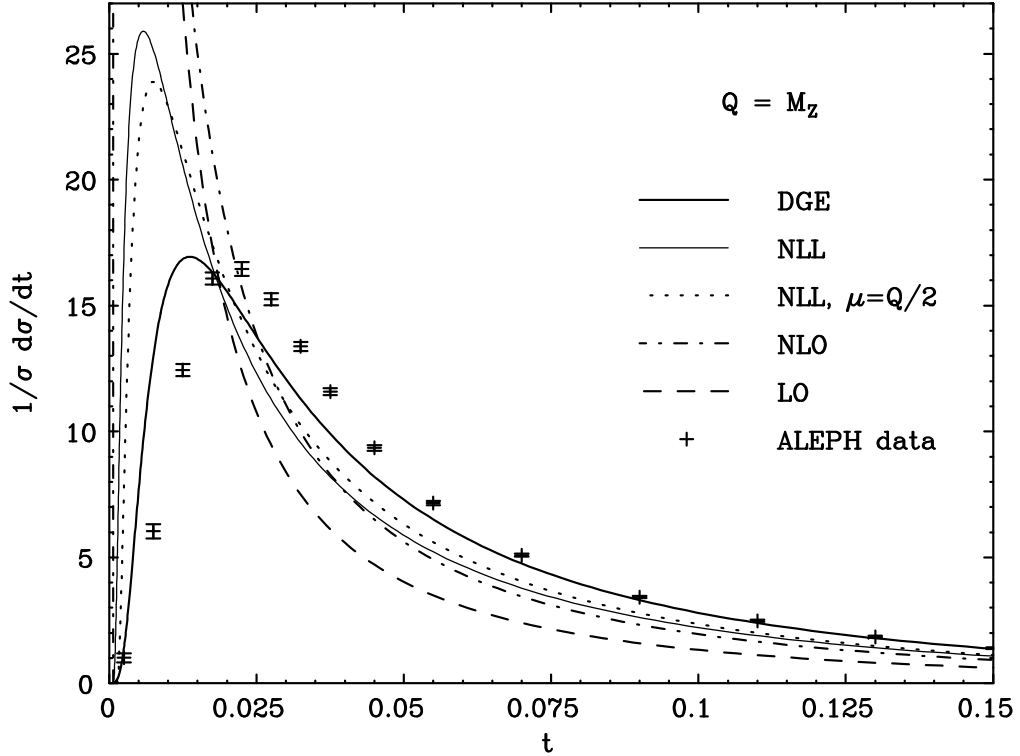


Figure 4: DGE, the standard NLL and the LO and NLO results as a function of t in the two-jet region, at $Q = M_Z$. Fixed-order and NLL results are in the $\overline{\text{MS}}$ scheme. As an example of scale dependence the NLL result is shown at two different renormalization points $\mu_R = Q$ and $\mu_R = Q/2$. For the LO and NLO results $\mu_R = Q$. We assume $\alpha_s^{\overline{\text{MS}}}(M_Z) = 0.110$. \aleph data [48] is shown for orientation.

ence between the NLO and the LO signals large higher-order corrections. So does the renormalization scale dependence of the result (not shown in the plot). The qualitatively different behaviour of the NLL result is clearly seen: thanks to exponentiation it vanishes at $t = 0$. Nevertheless, as fig. 4 shows, the renormalization scale dependence is still appreciable. We stress that the factor 2 between the renormalization points is completely arbitrary. This difference should *not* be considered as a reliable estimate of the error due to running coupling effects that have been neglected, since the physical scale, (e.g. the transverse momentum) in the two-jet region is significantly smaller than Q . As anticipated in sec. 3.2, the impact of the additional resummation of sub-leading logs by DGE is quite significant. Having performed this resummation, the renormalization scale dependence (at the level of the logarithmically enhanced cross-section) is avoided.

In fig. 4, as in all forthcoming calculations we use the so-called log-R matching scheme [6] to complement the calculation of the logarithmically enhanced cross-section. Using the known NLO calculation [10, 11], $R(Q^2, t) \equiv 1 + R_1(t)a + R_2(t)a^2 + \dots$ where $R_1(t)$ is known analytically and $R_2(t)$ is parametrised based on a numerical computation

by EVENT2 [11], we write

$$R(Q^2, t) = \exp \left\{ R_1 a(Q^2) + \left(R_2 - \frac{1}{2} R_1^2 \right) a(Q^2)^2 + \ln R(Q^2, t) \Big|_{\text{res}} - \ln R(Q^2, t) \Big|_{\text{res}}^{\text{NLO}} \right\}. \quad (106)$$

Here $\ln R(Q^2, t) \Big|_{\text{res}}$ is our resummed result for the logarithmically enhanced integrated cross-section, given by eqs. (64) and (63) and $\ln R(Q^2, t) \Big|_{\text{res}}^{\text{NLO}}$ is its expansion, up to NLO in $\overline{\text{MS}}$,

$$\begin{aligned} \ln R(Q^2, t) \Big|_{\text{res}}^{\text{NLO}} = & \left[-C_F L^2 + \frac{3}{2} C_F L \right] a(Q^2) + \left[-C_F \beta_0 L^3 \right. \\ & + \left(-\frac{11}{12} C_F \beta_0 - \frac{1}{3} \pi^2 C_F^2 + \left(\frac{1}{12} \pi^2 - \frac{1}{3} \right) C_A C_F \right) L^2 \\ & + \left(\frac{15}{4} C_F \beta_0 + \left(-4 \zeta_3 + \frac{1}{2} \pi^2 \right) C_F^2 + \left(\frac{1}{2} - \frac{1}{8} \pi^2 \right) C_A C_F \right) L \\ & \left. + \left(3 \zeta_3 - \frac{1}{180} \pi^4 - \frac{3}{16} \pi^2 \right) C_F^2 \right] a(Q^2)^2. \end{aligned} \quad (107)$$

The matching (106) is done in the $\overline{\text{MS}}$ scheme. Renormalization scale dependence appears only beyond the level of the logarithmically enhanced cross-section and it is therefore suppressed by t . Numerically, the residual scale dependence (see table 1) is very small as long as the log-enhanced cross-section dominates. The difference is much too small to be observed in the resolution of fig. 4. At large t ($t \gtrsim 0.2$) the terms which are suppressed by t start making an impact and eventually the scale dependence becomes comparable to its values in the NLL and the NLO results.

Table 1: Residual renormalization scale dependence: the relative difference between the differential cross-section at $Q = M_Z$ as calculated from (106) when the matching with the NLO result is performed at $\mu_R = Q$ and at $Q/2$.

t	0.02	0.05	0.10	0.15	0.20	0.25	0.30	0.33
%	0.22	0.16	0.02	0.29	0.62	1.20	3.0	7.5

Next, we confront the question of reliability of the approximation technique we used in section 3.3 in evaluating the Borel sum. In the calculation presented in fig. 4 we evaluated the Borel sum in (63) using $p_{\text{max}} = 8$. This means that the function $V(z)$ in eq. (52) was approximated by 8 poles. Note that p_{max} is also the largest power of $\ln \nu$ respected by this approximation (see (54)). In addition, the renormalon integrals $\tilde{I}_p(\ln Q^2/\bar{\Lambda}^2)$ were evaluated using the two-loop running coupling in the “gluon bremsstrahlung” scheme (see section 4). How sensitive are the results to these approximations? To answer this question we repeat the calculation varying the choice of p_{max} and the running coupling. Considering first the choice of p_{max} , we show in fig. 5 approximants of increasing order. The convergence is quite remarkable. In the upper plot the $p_{\text{max}} = 5$ curve (dashed) can hardly be distinguished from the $p_{\text{max}} = 8$ curve. Indeed, as the lower plot shows, the

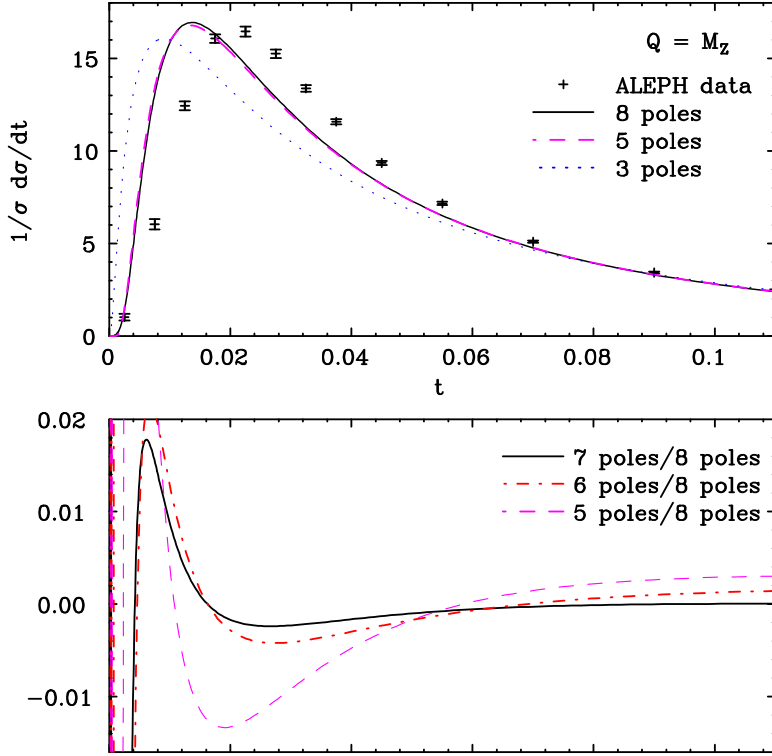


Figure 5: The convergence of increasing approximants to the perturbative cross-section, according to the technique of section 3.3, eq. (63). The upper plot shows the differential cross-section for $p_{\max} = 3, 5$ and 8 and the lower plot shows the relative error of the differential cross-section with respect to the $p_{\max} = 8$ calculation, for $p_{\max} = 5, 6$ and 7 . We fix $\alpha_s^{\overline{\text{MS}}}(M_Z) = 0.110$ and use two-loop running coupling; log-R matching is applied.

difference between them is very small and it exceeds 1% only around the distribution peak. For our fits, we choose $p_{\max} = 8$ which guarantees a truncation error^{††} of less than 1% down to $t = 0.01$ at M_Z (or $0.01 M_Z/Q$ at Q).

The stability of the calculation with respect to the running coupling can be checked by repeating the calculation with a different renormalization-group equation. In principle, one may also consider changing the definition of Λ , thus replacing the “gluon bremsstrahlung” coupling by some other coupling that matches the same Abelian limit. This was done in a similar context in the case of the average thrust [12]. It was found there that such a replacement introduces a non-negligible variation in the calculated observable, but the final impact on the extracted value of α_s was rather small (of order 1%). In the context of the distribution, the choice of the “gluon bremsstrahlung” coupling is almost imposed on us by consistency with the NLL exponentiation kernel. Therefore we shall not make such a modification. The simplest variation in the renormalization-group equation is to replace it by the one-loop. In this case the renormalon integrals $\tilde{I}_p(\ln Q^2/\Lambda^2)$

^{††}This is the error in evaluating the principle-value Borel sum, which is well defined mathematically. This truncation error must not be confused with the ambiguity of the perturbative sum.

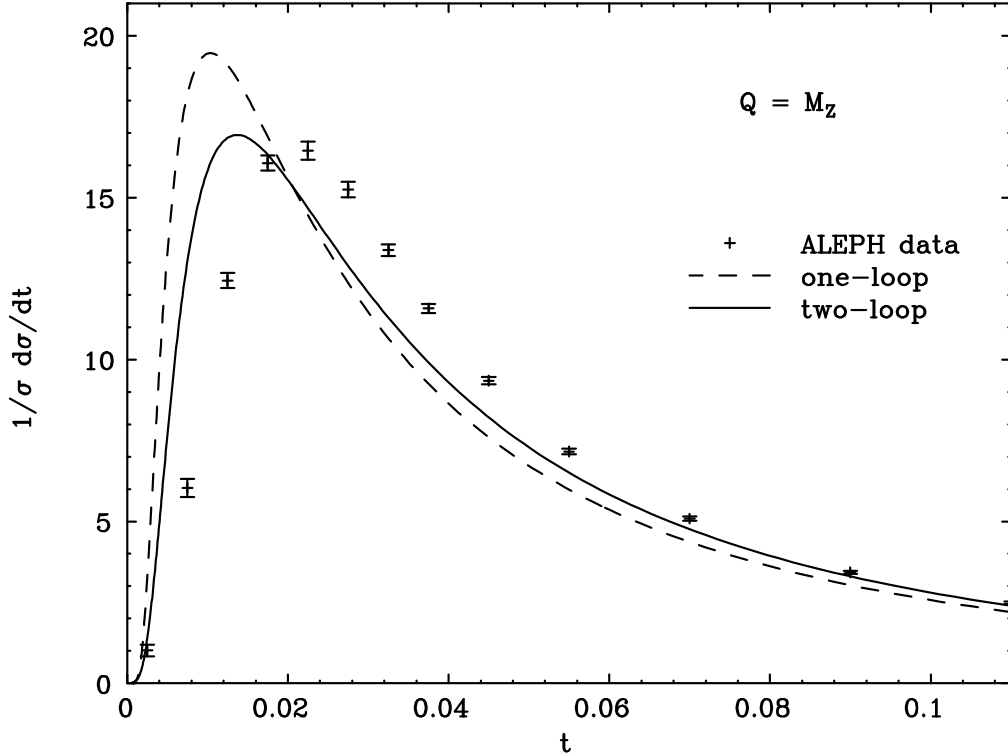


Figure 6: The resummed cross-section at M_Z based on one-loop (dashed) and two-loop (full line) running coupling. We fix $\alpha_s^{\overline{\text{MS}}}(M_Z) = 0.110$ and use $p_{\max} = 8$; log-R matching is applied. \aleph data [48] is shown for orientation.

are evaluated by eq. (60) instead of eq. (62). Such a comparison is presented in fig. 6.

The difference between the two curves is quite significant, in particular in the peak region. Note, however, that contrary to the two-loop case, the one-loop resummed result does not include all the next-to-leading logs (the terms proportional to β_1 are omitted). The difference between two- and three-loop* running coupling is expected to be much smaller. However, it may well be non-negligible close to the peak, so it is certainly worth consideration in the future. In the following we will use the two-loop running coupling.

5.2 Non-perturbative corrections

It was realized before [2, 23, 24, 25] that non-perturbative power corrections of the form $\lambda_n(\Lambda/tQ)^n$ to any power n become relevant around the distribution peak. As shown in section 3.5, such corrections are indeed expected based on the form of the ambiguity of the perturbative result. If all the powers are as important, one would need an infinite number of parameters – or a completely arbitrary shape-function – to bridge the gap between the perturbative result and the data. In practice one assumes that there is a

*In the spirit of [15] and our discussion in sec. 4, the appropriate value for β_2 should probably be set based on the NNLO coefficient of the singular term $1/(1-x)$ in the splitting function.

region in t where a power corrections expansion such as (90) is dominated by its first few terms, or in other words, that the shape-function can be described by its first few moments. It is therefore essential that λ_n do not grow too fast with n . Having made this assumption, one can put a cut t_L on the fitted range in t for any given energy, and fit the data for $t > t_L$ using a reasonably flexible parametrisation of the shape-function. This cut should scale like the distribution peak, i.e. as $1/Q$,

$$t_L(Q) = t_L(M_Z) \frac{M_Z}{Q}. \quad (108)$$

In any case, the dependence of the results on the precise location of this cut and on the specific functional form of the shape-function must not be too large.

The simplest possibility is to place the cut at large enough values of t such that the only relevant non-perturbative parameter will be λ_1 , which controls the shift of the distribution (87). This approach was suggested in [3]. The advantage is that the perturbative calculation is better under control and the “model dependence” in the parametrisation of non-perturbative corrections is minimized. The price, however, is that one does not use a large part of the data, and in particular, one excludes the region where the distribution changes sharply and is therefore expected to be most constraining and most informative.

Here we use various different minimal t cuts and perform fits where a flexible shape-function is convoluted with the perturbative distribution as well as fits with just a shift. For the shape-function-based fits the minimal cut can be quite low, thus using almost all available data. At the low end we choose $t_L(M_Z) = 0.01$. This is equivalent to $Qt \gtrsim 2\bar{\Lambda}$ and it guarantees convergence of the Borel function approximation within 1%, as shown in fig. 5. Less ambitious cuts $t_L(M_Z) = 0.02$ and 0.03 are useful to check the stability, which is indicative of whether the power-correction expansion is convergent enough. For the shift-based fit higher cuts must be used. Also here stability of the results is important to guarantee that sub-leading power corrections are not too relevant in the fitted range.

For simplicity we shall assume that the parameters of the shift or the shape-function are Q independent, even though we have shown that logarithmic dependence is expected in general. In principle, a fit that allows logarithmic dependence of λ_n according to eq. (84) is more appropriate. But, since κ_p are not known, the price will be having more parameters which can only be constrained by very precise data at *several different energies*. The available data is not constraining enough for such a fit.

5.2.1 Fits with a shifted distribution

Let us consider first a fit based on shifting the perturbative distribution. We use experimental data from all energies in the range $14 \text{ GeV} \leq Q \leq 189 \text{ GeV}$ (summarised in table 4 below). When available, the systematic errors have been added in quadrature to the statistical errors. Table 2 summarizes the fit results for α_s and λ_1 as a function of the low cut. First of all we note that the fits are very good: the χ^2/dof values are unusually low. Next, we see that the results depend on the low cut.

Particularly stable results, as far as the extracted value of α_s is concerned, are obtained for $t_L(M_Z) \gtrsim 0.07$. Above this value consecutive cuts yield α_s values that are

Table 2: Fits of α_s and λ_1 to data in the range $14 \text{ GeV} \leq Q \leq 189 \text{ GeV}$ with a lower limit $t_L(M_Z) Q/M_Z$ and upper limit $t_H = 0.32$. The last two columns show the obtained value of χ^2 per degree of freedom and the total number of data points used in the fit, respectively.

$t_L(M_Z)$	$\alpha_s^{\overline{\text{MS}}}(M_Z)$	λ_1	χ^2/dof	points
0.02	0.1072 ± 0.0002	1.60 ± 0.07	0.96	231
0.03	0.1066 ± 0.0003	1.78 ± 0.10	0.84	213
0.04	0.1072 ± 0.0004	1.51 ± 0.15	0.70	193
0.05	0.1080 ± 0.0005	1.19 ± 0.19	0.67	177
0.06	0.1089 ± 0.0006	0.83 ± 0.22	0.62	165
0.07	0.1096 ± 0.0008	0.54 ± 0.29	0.65	152
0.08	0.1099 ± 0.0009	0.44 ± 0.34	0.62	140
0.09	0.1105 ± 0.0011	0.20 ± 0.39	0.62	127
0.10	0.1110 ± 0.0015	0.02 ± 0.49	0.64	119
0.11	0.1115 ± 0.0022	-0.14 ± 0.61	0.63	109
0.12	0.1127 ± 0.0026	-0.51 ± 0.82	0.61	101
0.14	0.1119 ± 0.0040	-0.29 ± 1.63	0.60	91

within errors of each other. This stability means that sub-leading power corrections in this region are small enough to be neglected. Thus we regard the result $\alpha_s^{\overline{\text{MS}}}(M_Z) \simeq 0.110$ as reliable. Too high cuts $t_L(M_Z) \geq 0.10$ are disfavoured because the number of fitted points decreases significantly (note that the propagated experimental error increases accordingly). Cuts like $t_L(M_Z) = 0.05$ or 0.06 have the advantage of increased sensitivity to λ_1 . Lower cuts are probably too sensitive to sub-leading power corrections. This is reflected in the stronger dependence on the cut and in the deterioration of χ^2/dof . In the following we shall use $t_L(M_Z) = 0.05$ for illustrations. It has the additional advantage of consistency with the shape-function-based fit (see below).

The table and fig. 7 show that there is a strong correlation between α_s and λ_1 . A similar correlation was found in [3]. This means that quantitative discussion of the values of non-perturbative parameters, like λ_n is relevant only for a fixed α_s .

In all the fits discussed so far we used an upper cut $t_H = 0.32$ which is Q independent. We checked that the location of this cut does not influence the fit. For example, keeping the lower cut fixed $t_L(M_Z) = 0.05$ and changing the upper cut between $t_H = 0.29$ and $t_H = 0.35$ (corresponding to a total of 154 to 184 fitted points, respectively) the central value of α_s changes by just 0.2% (and that of λ_1 by 4%).

Figures 8 through 10 show the fitted distribution and the original perturbative distribution together with the experimental data. For large Q we show only the small t region, which is more interesting. The agreement between the shifted distribution and the data is good. Nevertheless, it is clear that around the peak additional corrections are required (in the case of M_Z , for example). Indeed we saw that such corrections are expected based on the renormalon ambiguity.

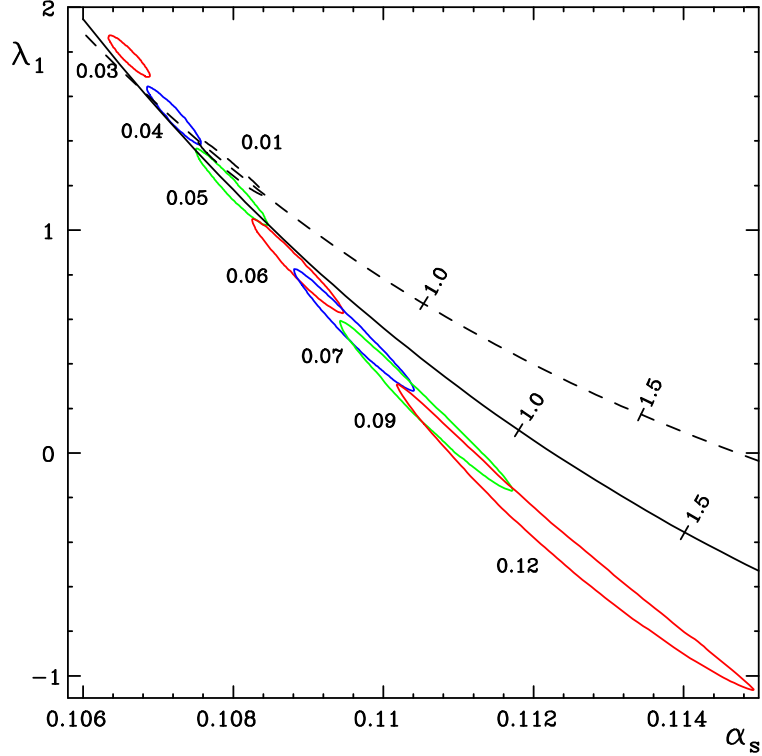


Figure 7: The correlation between α_s and λ_1 , as determined by a shift-based fit with various cuts (full one-sigma contours) and by a shape-function-based fit with a cut $t_L(M_Z) = 0.01$ (dashed one-sigma contour). The additional lines indicate the values of λ_1 in fits with a fixed α_s . The full line corresponds to the shift-based fit with $t_L(M_Z) = 0.05$ with and the dashed to the shape-function-based fit with $t_L(M_Z) = 0.01$. When α_s is free (the centre of the corresponding contour) $\chi^2/\text{dof} = 0.67$ and 0.86 , respectively. The points where $\chi^2/\text{dof} = 1$ and 1.5 are indicated.

5.2.2 Fits with a shape-function

Consider now a fit where the perturbative distribution is convoluted with a shape-function. According to sec. 3.5, this means, in fact, two convolutions: one with the large-angle shape-function $f_{\text{la}}(\epsilon)$, defined in eqs. (89) and (90), and another which corrects for the collinear contribution where we only include the leading term in (95),

$$f_{\text{col}}(Q^2, t) = \delta(t) - \lambda_2 \left[\frac{\bar{\Lambda}^2}{Q^2 t} \right]_+ \star \delta^{(1)}(t).$$

The main difference with previous works where a shape-function was used [25, 26] is in the starting point: the perturbative distribution there is the standard NLL result (with some cut-off regularization) while we start with the DGE result (regularized via the principal-value prescription) avoiding the truncation of sub-leading logs. The latter provides an analytic continuation of the perturbative treatment beyond its original range of applicability.

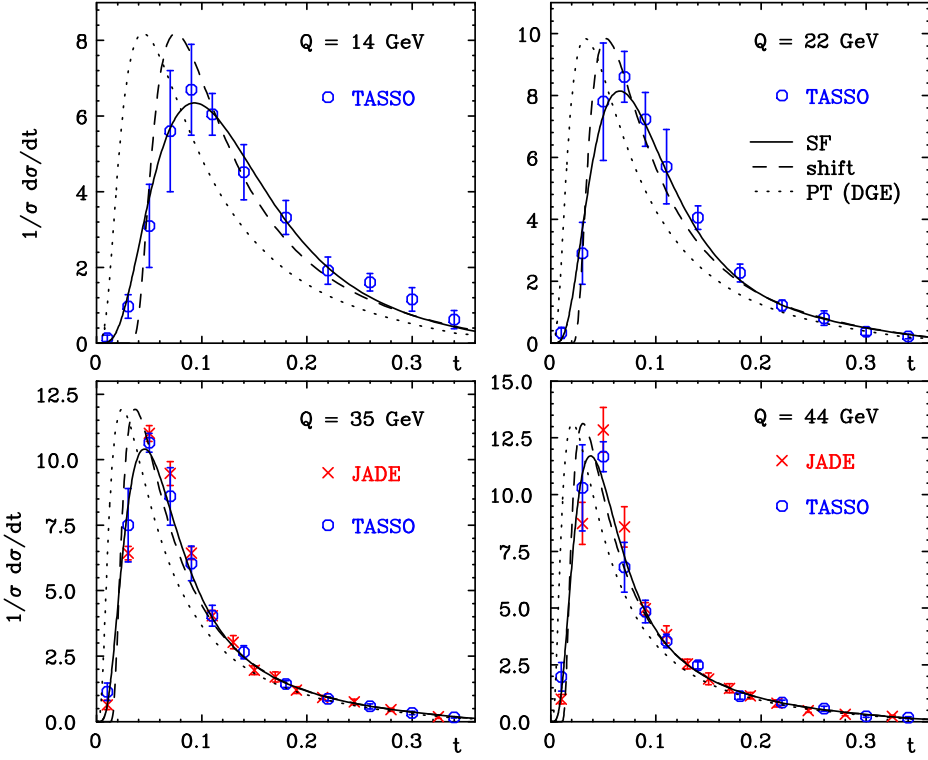


Figure 8: Comparison with experimental data at $Q = 14, 22, 35$ and 44 GeV with the perturbative calculation (dotted) and the corresponding fits using a shift (dashed) or a shape-function (full line). The perturbative calculation (DGE) is performed using principal-value Borel summation with two-loop running coupling. The fits are based on the range $t_L(M_Z) \frac{M_Z}{Q} < t < t_H = 0.32$, where $t_L(M_Z) = 0.05$ in the case of a shift and $t_L(M_Z) = 0.01$ in the case of the shape-function. The coupling is $\alpha_s^{\overline{\text{MS}}}(M_Z) = 0.108$, which is the best fit value in both cases.

In spite of the significant difference in the perturbative distribution as compared to [25, 26], we consider their ansatz for the shape-function appropriate also in our case, barring the fact that it is positive definite. To allow in principle the suppression of even moments as implied by our analysis in sec. 3.5, we consider a function that is flexible enough:

$$f_{\text{la}}(\epsilon) = n_0 \epsilon^q (1 + k_1 \epsilon + k_2 \epsilon^2) e^{-b_1 \epsilon - b_2 \epsilon^2} \quad (109)$$

where n_0 is fixed by the normalization requirement $\int f(\epsilon) d\epsilon = 1$ and q, k_1, k_2, b_1 and b_2 are free parameters to be fixed by the fit to the data. We assume $q > 0$ so that $f_{\text{la}}(0) = 0$ and $b_2 > 0$ (or $b_2 = 0$ and $b_1 > 0$) so that the shape-function decreases at large ϵ .

Note that with a shape-function of this form, the central moments λ_n do not have a definite sign. In particular both positive and negative values for λ_1 are possible. When a cut-off regularization is used it is intuitively clear that the shift is to the right: soft gluons widen the jets. Indeed λ_1 was found to be positive in both the shift-based fit in [3] and in the shape-function [25, 26] based fit. The shift parameter λ_1 was shown to

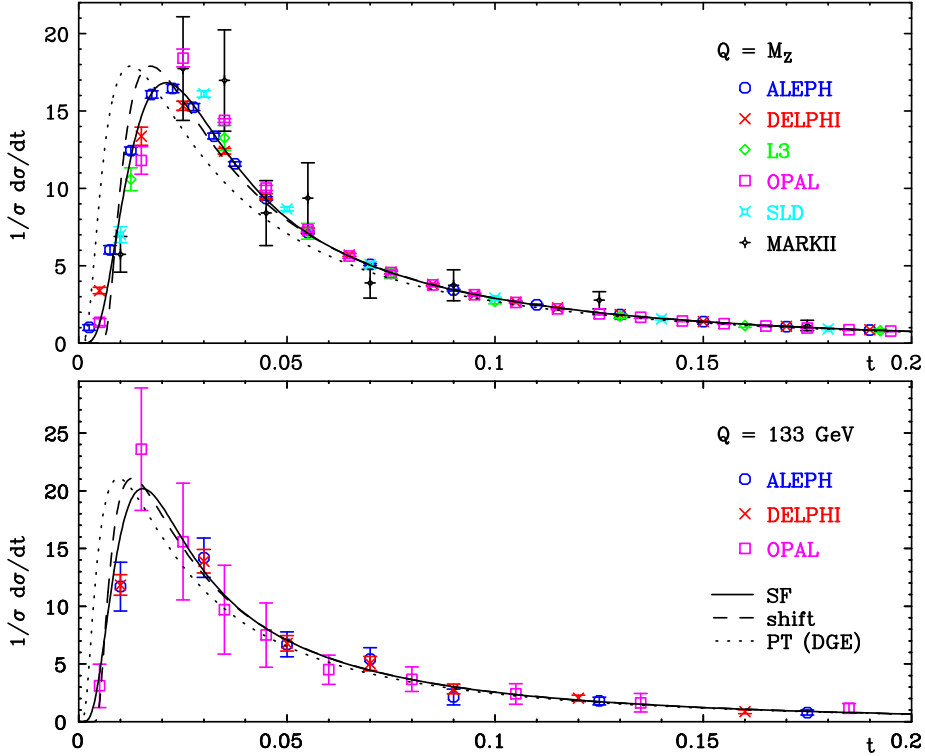


Figure 9: Comparison with experimental data at $Q = 91$ and 133 GeV with the perturbative calculation (dotted) and the corresponding fits using a shift (dashed) or a shape-function (full line). See fig. 8 for further details.

be roughly consistent with the leading power correction to average event-shapes [3, 32], which is always positive. The intuitive argument is not anymore valid when principal value regularization is used instead. According to [12], in this regularization λ_1 is still positive. We stress, however, that there is no general reason to exclude a priori the possibility of a negative λ_1 .

Performing a fit with $f_{la}(\epsilon)$ and the collinear correction (109) with a lower cut $t_L(M_Z) = 0.01$ and an upper cut $t_H = 0.32$, we obtained a very good fit with $\chi^2/\text{dof} = 0.86$ (for a total of 246 fitted data points). The fit results are shown in figures 8 through 10. The entire range of t is shown for all energies in fig. 11. The parameters in this case are

$$\begin{aligned}
 \alpha_s^{\overline{\text{MS}}} (M_Z) &= 0.1080 \pm 0.0004 \\
 q &= 0.533 \pm 0.083 \\
 b_1 &= 0.664 \pm 0.076 & k_1 &= -0.176 \pm 0.058 \\
 b_2 &= 0 & k_2 &= 1.9 \cdot 10^{-6} \pm 0.010
 \end{aligned} \tag{110}$$

corresponding to

$$\begin{aligned}
 \lambda_1 &= 1.28 \pm 0.13 \\
 \lambda_2 &= 0.68 \pm 0.53.
 \end{aligned} \tag{111}$$

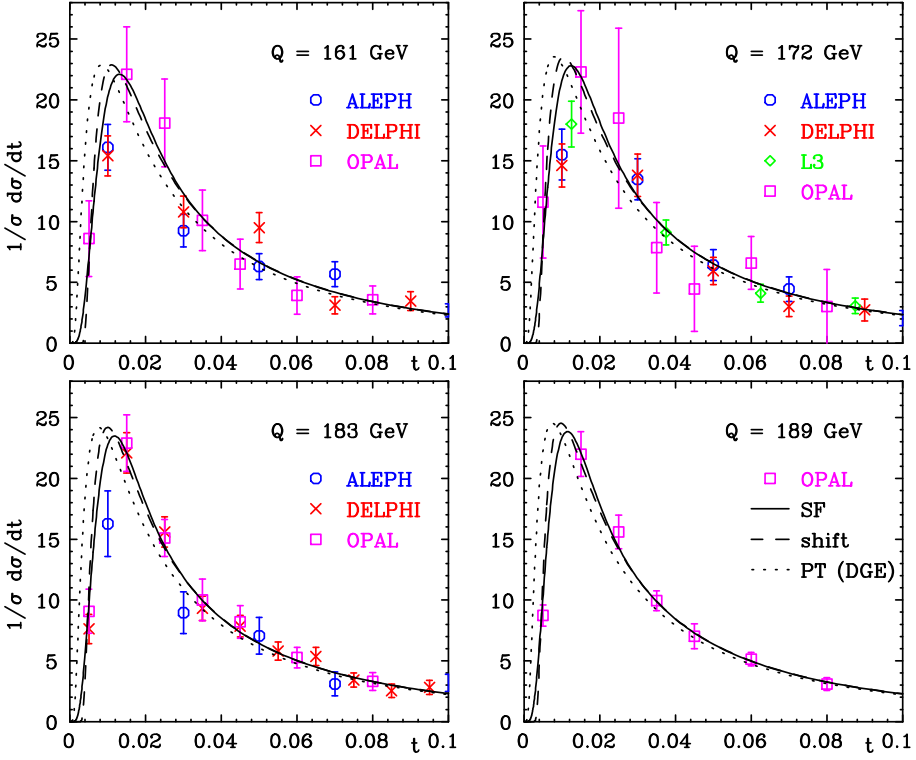


Figure 10: Comparison with experimental data at $Q = 161, 172, 183$ and 189 GeV with the perturbative calculation (dotted) and the corresponding fits using a shift (dashed) or a shape-function (full line). See fig. 8 for further details.

It turns out that the fit has a strong preference for a linear term in the exponent, so that if both b_1 and b_2 are free, then b_2 is set by the fit to zero. In order to try another functional form, thus testing the sensitivity of the fit results to the properties of the shape-function, we also fitted the data in the same range with the function where the linear term in the exponent is missing: $b_1 \equiv 0$. In this case we got a best fit with $\chi^2/\text{dof} = 0.92$, i.e. slightly worse than the previous one, with the following parameters,

$$\begin{aligned}
 \alpha_s^{\overline{\text{MS}}} (M_Z) &= 0.1068 \pm 0.0003 \\
 q &= 4.04 \pm 1.31 \\
 b_1 \equiv 0 & & k_1 &= -0.951 \pm 0.009 \\
 b_2 = 0.627 \pm 0.135 & & k_2 &= 0.222 \pm 0.005
 \end{aligned} \tag{112}$$

corresponding to

$$\begin{aligned}
 \lambda_1 &= 1.69 \pm 0.07 \\
 \lambda_2 &= -1.08 \pm 0.18.
 \end{aligned} \tag{113}$$

We see that most of the parameters of the shape-function are fairly well constrained by the fit. Unfortunately, this does not imply that the central moments of the shape-function are well determined. Note in particular that λ_2 changes sign between (111) and

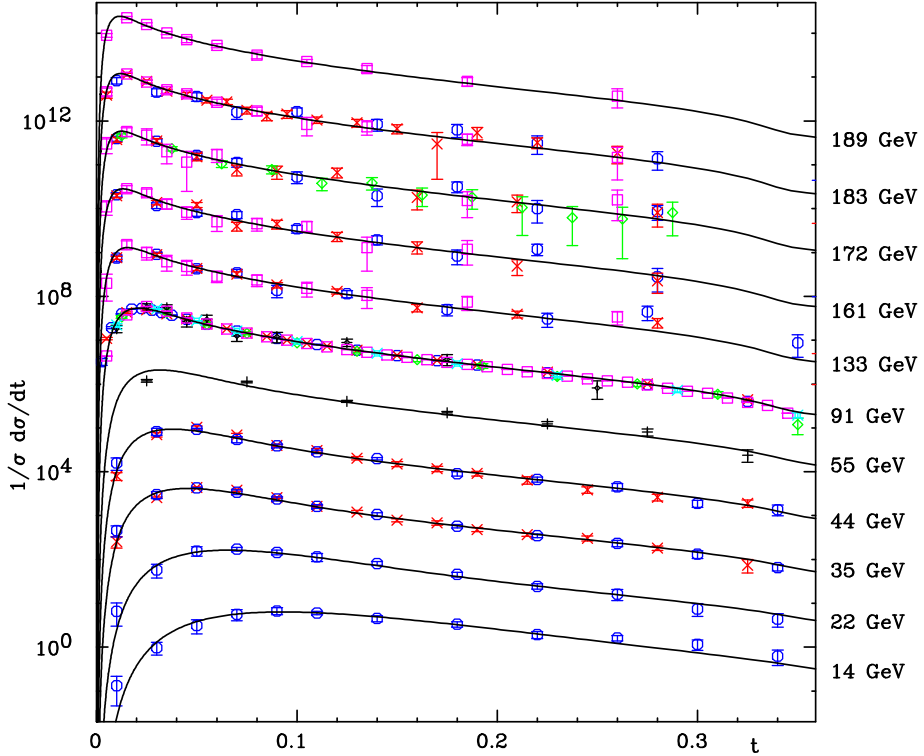


Figure 11: Comparison of DGE convolved with the best fit shape-function ($b_2 = 0$) with experimental data for $Q = 14$ up to 189 GeV. Here $\alpha_s^{\overline{\text{MS}}}(M_Z) = 0.108$. Data points with large errors ($\geq 100\%$) are not shown.

(113). As explained above, due to the correlation between α_s and the non-perturbative parameters, it makes sense to fix α_s in the fit when comparing the results for the two possible exponents. Doing so with $\alpha_s = 0.108$ we still obtain good fits in both cases. For a linear term in the exponent we get $\lambda_1 = 1.27 \pm 0.03$ ($\chi^2/\text{dof} = 0.86$) and for a square in the exponent we get $\lambda_1 = 1.34 \pm 0.02$ ($\chi^2/\text{dof} = 0.96$). Now the values of λ_1 are much closer. Note that also the propagated errors become smaller, since α_s and λ_1 are so strongly correlated.

Figure 7 shows how λ_1 varies when the fits with the shift and with the shape-function (with a linear term in the exponent) are performed with a fixed value of α_s . As intuitively expected, forcing a larger value of α_s , λ_1 decreases. For $\alpha_s^{\overline{\text{MS}}}(M_Z) \simeq 0.108$ similar values are obtained for λ_1 from the shift and from the shape-function (note that this depends on the chosen lower cut), however, for higher values of the coupling the values of λ_1 start differing. In this case the shape-function is not so well approximated by a δ -function (a shift) and its higher central moments λ_n play a role.

To allow a quantitative discussion concerning the higher central moments let us fix also λ_1 and compare the fits with the two exponents for the same α_s and λ_1 . We choose them to be the values obtained in our best fit (110): $\alpha_s^{\overline{\text{MS}}}(M_Z) = 0.108$ and $\lambda_1 = 1.28$.

Quantitative information on higher moments is theoretically important for several

reasons. First, it would be interesting to see the effect of the collinear contribution. At the same time it would be interesting to check our prediction that λ_2 (like other even central moments of the shape-function) is suppressed. Even ignoring the strong dependence on α_s , these two ingredients are hard to address by fitting the data: if λ_2 is small then the collinear correction is not important, and conversely – if the collinear correction is included a major part of the effect of λ_2 is cancelled, so λ_2 would be very hard to access. To deal with this we make three different fits with the same fixed values of α_s and λ_1 mentioned above: with the collinear correction, without it, and finally a fit where λ_2 is fixed to zero. The results are summarised in table 3.

Table 3: Determination of λ_2 and λ_3 for fixed $\alpha_s^{\overline{\text{MS}}}(M_Z) = 0.108$ and $\lambda_1 = 1.28$

	$b_2 = 0$			$b_1 = 0$		
with collinear	λ_2 0.64 ± 0.20	λ_3 -14.7 ± 2.7	χ^2/dof 0.85	λ_2 0.21 ± 0.17	λ_3 -7.1 ± 1.7	χ^2/dof 0.98
no collinear	0.64 ± 0.20	-14.9 ± 2.7	0.85	0.22 ± 0.16	-7.2 ± 1.5	0.98
$\lambda_2 \equiv 0$	0	-5.7 ± 2.7	0.89	0	-5.2 ± 0.5	0.99

The first conclusion is that λ_2 is not well determined by the fits: even for fixed values of α_s and λ_1 the two functional forms yield somewhat different results. Nevertheless, a vanishing λ_2 is certainly not inconsistent with the data: the fit does not deteriorate much by fixing it to zero. One also sees that the collinear correction is not important: including it or not leaves λ_2 almost identically the same. Had the value of λ_2 been significantly different from zero, such a situation would have been impossible, but for a small (and not very well constrained) λ_2 it is quite reasonable.

Table 3 also gives the λ_3 values. It is clear that λ_3 is not constrained enough unless α_s , λ_1 and λ_2 are all fixed. Still, one thing that can be said in general (varying the other parameters, including α_s) is that negative values for λ_3 are strongly preferred. Thus, a positive-definite ansatz for the shape-function (in the principal-value regularisation!) is not adequate. Note that the preferred signs of λ_1 (positive) and λ_3 (negative) are compatible with ρ_{2p}^{PV} being all positive (see eq. (80) and (84)).

We summarise in table 4 the contribution to χ^2 in the fit by each experiment separately. The middle columns correspond to a fit of the shifted distribution for α_s and λ_1 with a lower cut $t_L(M_Z) = 0.05$ and an upper cut $t_H = 0.32$. The columns on the right correspond to a fit for α_s and the parameters of the shape-function with a lower cut $t_L(M_Z) = 0.01$ and upper limit $t_H = 0.32$. The OPAL and SLD data sets at 91.2 GeV are not included in the fit since they are not consistent with the other data sets at this energy for small t . We note that there are no particular trends in the χ^2/point as a function of energy.

Table 4: Contribution to χ^2 in the two fitting procedures.

Experiment	Reference	Q [GeV]	χ^2 (shift)	points(shift)	χ^2 (SF)	points (SF)
TASSO	[45]	14.0	0.00	0	4.98	7
TASSO	[45]	22.0	1.37	2	3.28	8
JADE	[46]	35.0	3.77	6	29.80	11
TASSO	[45]	35.0	1.56	4	4.19	9
JADE	[46]	44.0	5.60	7	14.68	11
TASSO	[45]	44.0	9.07	5	13.00	9
AMY	[47]	55.0	2.45	4	10.82	5
ALEPH	[48]	91.2	4.26	10	9.82	17
DELPHI	[49]	91.2	11.23	13	17.77	17
L3	[50]	91.2	5.81	7	6.19	9
MARKII	[51]	91.2	7.27	6	9.51	9
OPAL	[52]	91.2	(26.62)	(27)	(284.41)	(31)
SLD	[53]	91.2	(9.02)	(6)	(96.03)	(8)
ALEPH	[54]	133.0	6.09	7	6.29	8
DELPHI	[55]	133.0	5.80	7	6.02	8
OPAL	[56]	133.0	2.70	7	3.49	10
ALEPH	[57]	161.0	5.64	7	12.44	8
DELPHI	[55]	161.0	9.88	7	12.14	8
OPAL	[58]	161.0	2.65	8	3.42	10
ALEPH	[57]	172.0	5.93	7	6.22	8
DELPHI	[55]	172.0	5.10	7	5.59	8
L3	[59]	172.0	3.79	10	4.13	11
OPAL	[60]	172.0	3.49	8	3.76	10
ALEPH	[61]	183.0	4.59	7	8.46	8
DELPHI	[55]	183.0	7.60	15	8.43	17
OPAL	[60]	183.0	0.96	8	1.41	10
OPAL	[60]	189.0	1.01	8	1.71	10
Sum			117.6	177	207.5	246

Finally, the shape-function-based fit can be considered an alternative way to extract the value of α_s . We saw already, that in spite of the fact that the determination of the non-perturbative parameters is far from being complete, α_s does not change much. In particular, for the two functions used, $\alpha_s^{\overline{\text{MS}}}(M_Z)$ varies only from 0.1068 to 0.1080. A further stability check is to what extent it is sensitive to the location of the low cut $t_L(Q)$. The answer is provided by table 5. The sensitivity to t_L in the determination of α_s is rather small. In particular it is smaller than in the case of a shift-based fit. There is still some tendency that α_s becomes larger for higher (thus less ambitious) cuts. While higher cuts are safer from the point of view suppressing sub-leading power corrections, they are less constraining as far as the multi-parameter shape-function is concerned. Note also that

Table 5: Fits of α_s and the shape-function (with a linear term in the exponent, $b_2 = 0$) as a function of the lower cut $t_L(Q)$. The upper cut is $t_H = 0.32$.

$t_L(M_Z)$	$\alpha_s^{\overline{\text{MS}}}(M_Z)$	λ_1	λ_2	χ^2/dof	points
0.010	0.1080 ± 0.0004	1.28 ± 0.13	0.68 ± 0.53	0.86	246
0.015	0.1083 ± 0.0005	1.22 ± 0.14	1.07 ± 0.55	0.83	241
0.020	0.1089 ± 0.0006	1.09 ± 0.14	1.62 ± 0.59	0.74	231
0.030	0.1098 ± 0.0008	0.95 ± 0.15	1.96 ± 0.64	0.70	213
0.040	0.1099 ± 0.0012	0.94 ± 0.18	1.77 ± 0.67	0.63	193
0.050	0.1091 ± 0.0016	1.05 ± 0.32	2.25 ± 0.96	0.63	177

the propagated experimental error on α_s and λ_1 increases for higher cuts. “Ambitious cuts” where the peak region itself is included in the fit, e.g. $t_L(M_Z) = 0.010$, are therefore favoured. We conclude that according to the shape-function-based fit $\alpha_s^{\overline{\text{MS}}}(M_Z)$ ranges between 0.107 and 0.110. These variations should be considered part of the theoretical uncertainty.

5.3 Moments of the thrust distribution

Given the assumption that the first few moments of the thrust $\langle t^n \rangle$ are dominated by the two-jet configuration, and therefore by the logarithmically enhanced cross-section, one can relate [24, 25] the parameters λ_n to the power corrections of the moments:

$$\begin{aligned} \langle t \rangle_{\text{two-jet}} &\simeq \langle t \rangle_{\text{PT}} + \lambda_1 \bar{\Lambda} / Q \\ \langle t^2 \rangle_{\text{two-jet}} &\simeq \langle t^2 \rangle_{\text{PT}} + 2\lambda_1 \langle t \rangle_{\text{PT}} \bar{\Lambda} / Q + \lambda_2 \bar{\Lambda}^2 / Q^2. \end{aligned} \quad (114)$$

These predictions have been compared in [27] with the power correction from a *single* gluon emission, based on the characteristic function (17),

$$\begin{aligned} \langle t \rangle_{\text{SDG}} &\simeq \langle t \rangle_{\text{PT}} + \lambda \bar{\Lambda} / Q + \mathcal{O}(\bar{\Lambda}^3 / Q^3) \\ \langle t^2 \rangle_{\text{SDG}} &\simeq \langle t^2 \rangle_{\text{PT}} + \mathcal{O}(\bar{\Lambda}^3 / Q^3). \end{aligned} \quad (115)$$

The assumption that the two-jet region is dominant probably holds for the average thrust. The immediate conclusion is that the shift of the distribution λ_1 must coincide with the leading power-correction for the average, λ . The latter was determined from a fit in [12] using the principal value Borel sum regularization. For $\alpha_s^{\overline{\text{MS}}}(M_Z) = 0.110$, which is the best fit value in the case of the average thrust, $\lambda \bar{\Lambda} = 0.62 \pm 0.12$ GeV. This number can be compared with our current fits to the distribution with a fixed $\alpha_s^{\overline{\text{MS}}}(M_Z) = 0.110$. We get $\lambda_1 \bar{\Lambda} = 0.23 \pm 0.02$ GeV in a shift-based fit with a cut $t_L(M_Z) = 0.05$ (corresponding to $\chi^2/\text{dof} = 0.77$ for 177 points) and $\lambda_1 \bar{\Lambda} = 0.32 \pm 0.01$ GeV with a shape-function-based fit with a cut $t_L(M_Z) = 0.01$ (corresponding to $\chi^2/\text{dof} = 0.95$ for 246 points). The power correction extracted from the distribution is therefore lower than the corresponding power correction extracted from $\langle t \rangle$. The main reason for the discrepancy is the difference

between the resummation procedures used in the two cases. In the case of the distribution DGE is used, where the exponentiation plays a major role but terms that are suppressed by t are neglected. On the other hand in case of the average a *single* dressed gluon renormalon sum is used, where terms that are suppressed by t (and higher powers) are included but multiple gluon emission is neglected (apart from the NLO term).

An even more difficult case is that of the second moment $\langle t^2 \rangle$. As explained in [27], the absence of the term $2\lambda_1 \langle t \rangle_{\text{PT}} \bar{\Lambda}/Q$ in (115) is an artifact of using the single gluon approximation. On the other hand the absence of the term $\lambda_2 \bar{\Lambda}^2/Q^2$ is physically meaningful (a SDG analysis is the appropriate tool to identify such a power-correction, if it exists). Our current finding that the effect of λ_2 is cancelled at the level of the distribution is consistent with that of eq. (115). It is interesting to note, however, that eq. (115) was derived in [27] based on the entire characteristic function, while our current conclusion concerning λ_2 is based on the logarithmically enhanced cross-section alone. If two-jet dominance applies to $\langle t^2 \rangle$, fixing λ_1 and λ_2 by the distribution would allow the determination of the power-corrections to $\langle t^2 \rangle$ based on (114). Unfortunately, this is too optimistic: as one can verify, e.g. by looking at the data for the distribution scaled by t^2 (see [43]), at M_Z this observable gets a significant contribution from the region $t \gtrsim 0.2$. As we saw at various stages of the current investigation (see e.g. fig. 20 and table 1) the logarithmically enhanced cross-section ceases to dominate at $t \gtrsim 0.2$. It follows that the second moment of the thrust depends on contributions we neglected here. Perturbative and non-perturbative physics of three jets[†], including terms that are sub-leading in t at NNLO, must be taken into account for a reliable analysis of this quantity.

5.4 Theoretical uncertainty

As always, there are unproven assumptions and various limitations to our approach. Here we address several issues shortly. A quantitative analysis is restricted to those approximations we have made where a particularly significant impact on the extracted value of α_s is expected.

First in line is the uncertainty in the perturbative calculation. Here there are two major issues: the first is the uncertainty due to missing NNLO calculations. The significance of NNLO corrections was emphasized recently in [40]. In our analysis it is reflected for instance in the large renormalization scale dependence in the region $t \sim 1/3$. Once such a calculation is available, matching with the DGE would allow a significant reduction in the uncertainty, in particular, concerning the extraction of α_s . The second issue concerns exponentiation: the DGE performed here is only approximate beyond NLL. An exact NNLL calculation would allow one to test certain aspects of this approach and complement the resummation.

Concentrating on the two-jet region we neglected effects that are explicitly suppressed by t , but renormalon factorial growth is not restricted to the logarithmically enhanced terms. Large numerical coefficients appear also in the “remainder function”. Fig. 1 shows that at $t \simeq 0.2$, such sub-leading terms become important. Eventually, DGE may be

[†]Recently, non-perturbative effects in three-jet observables were addressed [41].

generalized to included them. Currently it is not known whether these terms exponentiate or not (and therefore they are treated differently in different “matching schemes”). One can give an estimate of the possible impact of such terms by making a modification of the log, as suggested in [6], e.g. $\ln 1/t \rightarrow \ln(1/t - 1)$. Such a modification ensures that the logarithmically enhanced cross-section will vanish at $t = 1/2$, like the physical cross-section, rather than at $t = 1$. Some results for a shift-based fit are summarized in table 6.

Table 6: Fits of α_s and λ_1 to data with a modified log. The upper limit is $t_H = 0.32$. The results are presented as a function of the lower limit.

$t_L(M_Z)$	$\alpha_s^{\overline{\text{MS}}}(M_Z)$	λ_1	χ^2/dof	points
0.02	0.1084 ± 0.0003	1.30 ± 0.07	1.26	231
0.03	0.1081 ± 0.0003	1.35 ± 0.08	1.21	213
0.04	0.1095 ± 0.0005	0.88 ± 0.14	1.05	193
0.05	0.1110 ± 0.0006	0.42 ± 0.16	0.97	177
0.06	0.1125 ± 0.0009	-0.01 ± 0.19	0.92	165
0.07	0.1138 ± 0.0009	-0.33 ± 0.20	0.94	152
0.08	0.1141 ± 0.0012	-0.41 ± 0.23	0.95	139
0.09	0.1143 ± 0.0015	-0.43 ± 0.32	0.97	127
0.11	0.1141 ± 0.0016	-0.37 ± 0.33	0.99	109

The general quality of these fits is worse than in the case of the non-modified log, table 2. In addition there is a stronger dependence of α_s on both cuts. These two facts suggest that such a modification is not quite the appropriate way to take into account the fact that the physical cross-section vanishes at $t = 1/2$. Still, as a rough measure of the impact of the terms we neglected these results are useful. For the favoured cuts the difference in α_s is quite appreciable. It changes from ~ 0.110 to ~ 0.114 . A similar study for the shape-function-based fit (with $t_L(M_Z)$) shows a somewhat smaller change in α_s : the central value changes from ~ 0.108 to ~ 0.111 . Altogether we see that NNLO (and higher order) terms which are not logarithmically enhanced have a relatively significant impact on α_s . We consider this as the largest source of uncertainty.

One aspect in which the DGE may be improved is the running coupling formula. Our entire analysis was performed with a two-loop running coupling. The comparison with the one-loop case in fig. 6 shows a relatively large variation. We expect the difference between three-loop and two-loop to be much smaller, but it may be non-negligible.

Next, there are uncertainties in the way hadronization corrections are treated. Here we assumed that the dominant non-perturbative corrections appear in a way that matches the ambiguity in the perturbative calculation. The success this general approach has had in event-shapes and elsewhere is encouraging. However, here we take it one step further: we assume that the ν dependence of each renormalon ambiguity (not only the first!) is reflected in the dependence of the corresponding non-perturbative corrections. Of course, any assumption we took in the perturbative calculation may have an impact

on the prediction. In particular,

- Having neglected effects that are explicitly suppressed by t in the perturbative calculation, we cannot expect the power correction analysis to be reliable beyond $\mathcal{O}(1/t)$ accuracy.
- Since exponentiation is based on two-jet kinematics, non-perturbative effects that are associated with three jets (where the recoil of the quark must be taken into account) are not included.
- The normalization of the thrust variable by the sum of energies (Q) in (14) (rather than by the sum of the absolute values of the three-momenta) was shown to affect the coefficient of the leading power-correction in the case of the average thrust [4, 1]. There is a similar impact on the $1/Qt$ correction in the case of the distribution, and probably also on higher power corrections.
- Having neglected the non-inclusive decay of the gluon in the perturbative calculation in sec. 2, the effect is missed also on the non-perturbative level. See discussion below eq. (25).
- In our framework it is very natural to treat non-perturbative corrections as if they all exponentiate, since the perturbative calculation indicating their necessity is a calculation of the exponent. This is most clearly put in eq. (67): the ambiguity appears in the exponent and so should be the power corrections. It is probably true that in the peak region, the leading power corrections indeed exponentiate, but in general there are power corrections that do not.

There are also hadronization effects that cannot be associated with ambiguities in the perturbative calculation. For example, the latter does not contain information on the spectrum of the hadrons produced. In a recent work Salam and Wicke [42] showed that hadron mass effects introduce important corrections, for average values of event-shape variables.

Another fact we ignored here is that in reality also heavy quarks are produced. Since the data contains all events whereas in the calculation the quarks are treated as massless, some systematic error is expected.

6 Conclusions

Many infrared safe observables in QCD are sensitive to soft and collinear gluon radiation. This sensitivity appears at the perturbative level in the form of large Sudakov logs. In order to deal with this situation one must perform resummation of the logarithmically enhanced cross-section. The resummation has two aspects: exponentiation and integrals over the running coupling. The Dressed Gluon Exponentiation (DGE) differs from previous resummation methods in the way the second aspect is addressed. The approach makes a direct link between the resummation of Sudakov logs and that of infrared

renormalons. We showed that a careful treatment of running coupling integrals makes it possible to take into account a large class of logs, which is fully consistent with both the exact exponent up to NLL accuracy and renormalization group invariance. The latter is realized only when all the powers of the log are resummed. Moreover, sub-leading logs are factorially enhanced compared to the leading ones. As a consequence the standard approximation based on keeping the leading and the next-to-leading logs alone is not always justified.

DGE is a method to calculate a well defined class of log-enhanced terms based on exponentiation of the Single Dressed Gluon (SDG) renormalon-sum. The basic idea is that the exponent can be represented in terms of an integral over an observable-dependent characteristic function times the running coupling, similarly to the standard dispersive approach in renormalon calculations [1, 22]. This representation is natural since the exponentiation kernel is primarily associated with a single gluon emission. The method is quite general and can readily be applied to other physical quantities. The first stage is to calculate analytically the large N_f or massive gluon characteristic function, and then to identify the phase-space limits in the integration over the gluon virtuality as well as the specific terms in the characteristic function that contribute to logarithmically enhanced terms in the perturbative coefficients. This allows to obtain the logarithmically enhanced part of the SDG cross-section to all orders. At the next stage the physical cross section is obtained by exponentiating the SDG result. In the case considered here this exponentiation is rather straightforward, given the assumption that gluons are emitted independently from the quarks and contribute additively to 1 – thrust. In making this assumption we ignored correlations in multi-gluon emission that occur at higher orders. As a result, the exponentiation is only approximate as far as sub-leading logs (NNLL and beyond) are concerned. DGE cannot replace the construction of the exact exponent as a solution of the evolution equation up to a given logarithmic accuracy. It is rather complementary to it, similarly to the way resummation in general is complementary to fixed-order calculations.

One of the main results of this work is the observation that sub-leading Sudakov logs are factorially enhanced compared to the leading logs. This observation was made first at the level of the SDG cross-section, before exponentiation. At this level factorial growth appears only due to the collinear limit of phase space. The Borel function (in the large β_0 limit) has simple poles at $z = 1$ and 2 . However, the Borel integral is still well defined thanks to the analytic continuation. A much more dramatic factorial growth appears at the level of the exponentiated result in the Laplace conjugate variable ν . Here both the collinear and large-angle (soft) limits of phase space contribute to infrared renormalons. As a result of the large-angle contributions, the first infrared renormalon appears at $z = 1/2$, thus enhancing the divergence of the perturbative expansion as well as the relative significance of sub-leading logs compared to the leading logs. In the standard exponentiation formula [6] the most prominent enhancement of sub-leading logs, associated with the $z = 1/2$ renormalon, appear due to the leading term in the splitting function, the same term that generates the leading logs.

The traditional formulation of resummation is based on writing the exponent as an expansion in the coupling, with coefficients $g_n(\xi)$ that are functions of the combination

$\xi \equiv L\beta_0\alpha_s/\pi$, as in (3) (or in (46)). This way of organising the expansion is convenient when working with a fixed logarithmic accuracy. In this formulation, the enhancement of sub-leading logs translates into the properties of $g_n(\xi)$: these functions become more singular at $\xi = 1/2$ and $\xi = 1$ as n increases, and in addition they increase factorially. As was shown in fig. 3, the convergence of the expansion (46) depends strongly on the coupling (and thus on Q^2). In the case of the thrust sub-leading logs are quite important at all relevant energies. When using DGE and keeping all the logs the standard way of organizing the expansion loses its attractiveness: as a consequence of the factorial divergence of the functions $g_n(\xi)$ at large n the series must be truncated. Truncation at the minimal term would minimise the error, but this is not practical since the enhanced singularity of increasing order functions implies that the truncation order must itself be a function of L . An elegant alternative was presented in section 3.3: the exponent can be written in terms of a finite set of analytic functions $I_p(\ln Q^2/\bar{\Lambda}^2)$ with coefficients \bar{r}_p that are polynomials in L . Each function $I_p(\ln Q^2/\bar{\Lambda}^2)$ corresponds to a single renormalon integral over a simple or a double pole. In this way running coupling effects are resummed first and the logs only later. As was shown in fig. 5, the convergence of this resummation method is quite remarkable.

The ambiguities of the perturbative result obtained by DGE can be used as a template for the non-perturbative power corrections. In particular, we saw that it is possible to identify the t dependence associated with each renormalon singularity in the exponent. The leading power-correction for $t \gg \bar{\Lambda}/Q$ scales as $1/Q$. It corresponds to a simple renormalon pole at $z = 1/2$, with an ambiguity which is proportional to $1/t$. This results, upon exponentiation, in a shift of the distribution, as predicted by [2, 23, 3]. The physical origin of this correction is the sensitivity of the thrust to large-angle soft gluon emission. The same sensitivity gives rise to other renormalon singularities that are further away from the origin. The corresponding ambiguities scale as $\sim \bar{\Lambda}^n/Q^n$ and are therefore less important at large t . However, at small t they behave as $1/t^n$, implying non-perturbative corrections of the form $\lambda_n \bar{\Lambda}^n/(Qt)^n$. As emphasised by Korchemsky and Sterman, these corrections are all important in the distribution peak region. Since they exponentiate, it is natural to describe them by a non-perturbative shape-function. The parameters λ_n then correspond to the central moments of this function.

Our calculation shows that the ambiguities $\sim \bar{\Lambda}^n/Q^n$ with $n = 2, 4, \dots$ vanish in the large β_0 limit. This strongly suggests that the parameters λ_n for even n are suppressed according to eq. (84). In addition, the appearance of a double renormalon pole at $z = 1$ leads to a collinear power correction proportional to $\lambda_2 \bar{\Lambda}^2/(Qt)^2$, which has the opposite sign to the λ_2 term in the large-angle contribution. This leads to an almost complete cancellation of the overall effect of λ_2 .

The immediate phenomenological implication of these findings is that by shifting the distribution one should be able to fit the data in a wider range (closer to the peak) than a priori expected: there is no new effect beyond that of the shift so long as $\frac{\lambda_3}{\lambda_1} \frac{\bar{\Lambda}^2}{Q^2 t^2} \ll 1$, instead of $\frac{\lambda_2}{\lambda_1} \frac{\bar{\Lambda}}{Qt} \ll 1$. The phenomenological analysis indeed shows very successful shift-based fits, even for rather low t values (this was first observed in [3]). Clearly, in the peak region itself, a shift is not enough, and a convolution with a shape-function must

replace it.

Finally, our main conclusions from the phenomenological analysis can be summarised as follows: we obtained good fits based on the DGE result both with a shifted distribution and with a shape function. The two methods are fairly consistent with each other. This demonstrates that the data in the peak region can be used to extract α_s provided the appropriate resummation is performed and the power corrections are included. In the fits, the central value of $\alpha_s^{\overline{\text{MS}}}(M_Z)$ ranges between 0.107 and 0.114. The most important factor which limits the determination of α_s is the absence of a NNLO calculation. In particular, terms that are explicitly suppressed by t at NNLO are important, as can be deduced from the fact that the modification of the log: $\ln 1/t \longrightarrow \ln(1/t - 1)$ can change the extracted $\alpha_s^{\overline{\text{MS}}}(M_Z)$ by 4%. There are also non-negligible differences (3%) between different fitting procedures, such as dependence on the low t cut, the use of a shift or a shape-function, and the parametric form of the latter. Other factors contributing to the uncertainty are discussed in sec. 5.4.

The correlation between the non-perturbative parameters λ_n and α_s is strong. Consequently a quantitative discussion is restricted to the case where α_s is fixed. Then the shift parameter, or the first moment of the shape function, λ_1 is reasonably well determined (see fig. 7). Even when a modified log is used, the value of λ_1 as a function of α_s remains roughly the same. The sub-leading power-corrections are harder to constrain by the data. To determine the higher central moments of the shape-function it is useful to fix also λ_1 . As an example, fixing α_s and λ_1 to their best fit values we find that λ_2 is small and that the fit is not affected much by fixing it to zero (see table 3). Thus our theoretical prediction that the effect of λ_2 is small can be consistent with the data. A clear preference of the fits for a shape-function which is not positive-definite was observed.

Acknowledgments

We would like to thank Stefano Catani, Gregory Korchemsky and Gavin Salam for very interesting and useful discussions and Otmar Biebel and Stefan Kluth for useful correspondence.

A Numerical calculation of the NNLL part of the NLO coefficient

To calculate the NNLL part of the NLO coefficient we have used the EVENT2 [11] program. Writing the thrust-distribution on the form

$$\frac{1}{\sigma_0} \frac{d\sigma}{dL}(Q^2, L) \Big|_{\text{NLO}} = \mathcal{A}(L)a(Q^2) + \mathcal{B}(L)a(Q^2)^2,$$

where $L = \ln(1/t)$, $a = \alpha_s^{\overline{\text{MS}}}/\pi$, and $\mathcal{A}(L)$ is the analytically known leading order coefficient, the program calculates the next-to-leading order coefficient $\mathcal{B}(L)$ in the $\overline{\text{MS}}$ scheme using Monte Carlo integration. The program is written such that the different colour factor parts can be calculated separately (this was done first in [38]) in the following way,

$$\mathcal{B}(L) = C_F^2 \mathcal{B}_{C_F}(L) + C_F C_A \mathcal{B}_{C_A}(L) + C_F T_F N_F \mathcal{B}_{T_F}(L).$$

Since we are interested in the large L (small t) region we decreased the invariant mass cut-off on any pair of partons, $m_{ij}^2 > \text{CUTOFF}Q^2$, in the program to 10^{-14} from the default 10^{-8} in order not to restrict the phase-space for small t . To increase the sampling of the small t region we also changed the parameters NPOW1 and NPOW2 to 4 instead of the default values 2. The calculations presented below are based on 10^9 events (samplings of the integral). We used a linear binning in L and the bin size was chosen to be $\Delta L = 0.5$.

For each bin in L the Monte Carlo integration gives the integrated cross-section. From these integrals we then subtract the known NLL parts and normalise to the bin size giving the following integrals for each bin,

$$I_i = \frac{1}{\Delta L} \int_{L_{\min}}^{L_{\max}} (\mathcal{B}_i(L) - \mathcal{B}_i^{\text{NLL}}(L)) dL,$$

where $i = C_F, C_A, T_F$, and

$$\begin{aligned} \mathcal{B}_{C_F}^{\text{NLL}}(L) &= 2L^3 - \frac{9}{2}L^2 + \left(\frac{13}{4} - \pi^2\right)L, \\ \mathcal{B}_{C_A}^{\text{NLL}}(L) &= -\frac{11}{4}L^2 + \left(\frac{\pi^2}{6} - \frac{169}{72}\right)L, \\ \mathcal{B}_{T_F}^{\text{NLL}}(L) &= L^2 + \frac{11}{18}L. \end{aligned}$$

The results for the different integrals are shown in fig. 12. If it were not for sub-leading corrections, the integrals I_i would coincide with the NNLL coefficients $\mathcal{B}_{i,1}$. In principle one could take into account sub-leading terms by fitting a more general form to the integrals I_i . We choose instead to estimate a systematic error from sub-leading corrections for each bin in L . The estimate is based on assuming that the most important form of sub-leading corrections has the same power of logs as the leading log multiplied by one factor of t . The size of the coefficient multiplying this term is then assumed to be the

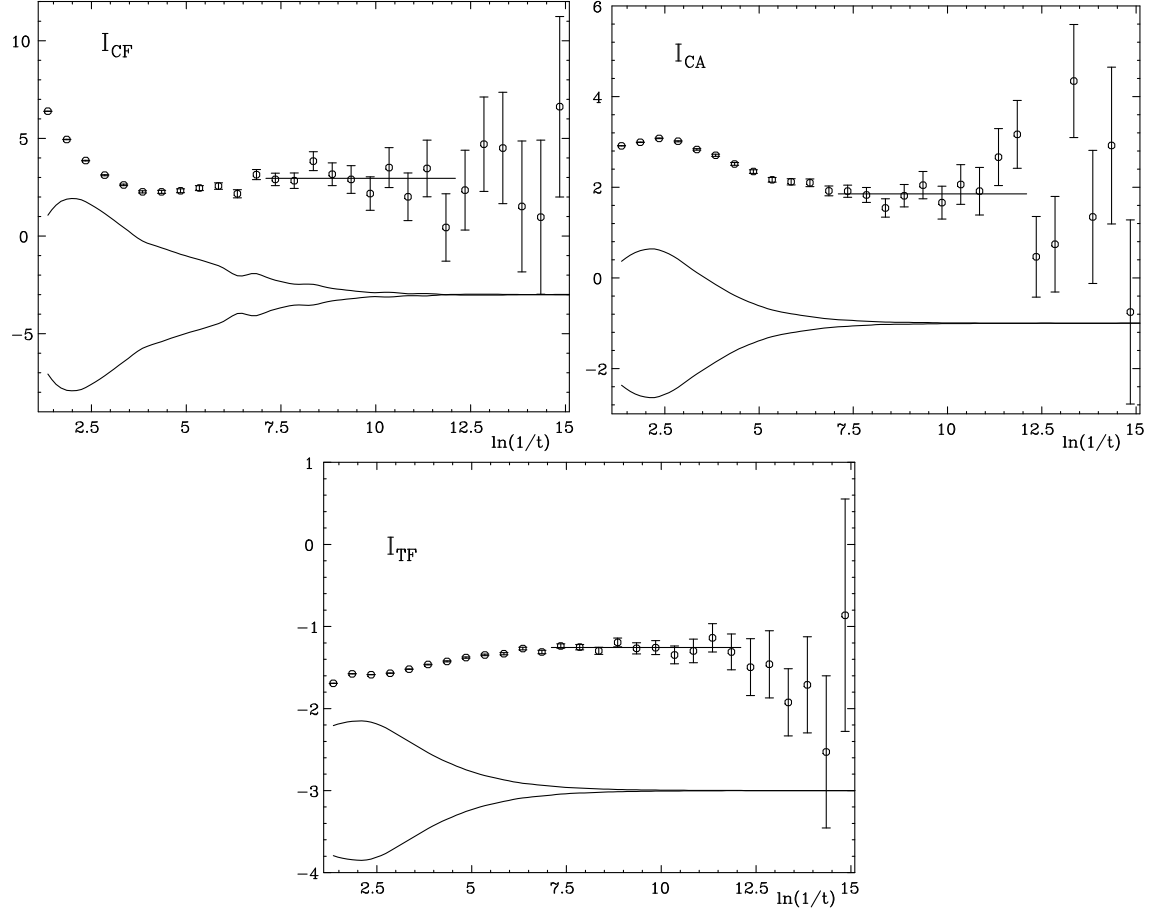


Figure 12: Results of the numerical calculation of the NLO coefficients \mathcal{B}_i with the NLL terms subtracted for the different colour factors. The band shows the estimated systematic error from sub-leading corrections when extracting the NNLL coefficients. The results of the fits are shown as straight lines in the regions fitted.

same as $\mathcal{B}_{i,1}$ estimated from the integral I_i . The systematic error for each bin is thus estimated by, e.g.

$$\Delta I_{CF} = \frac{I_{CF}}{\Delta L} \int_{L_{\min}}^{L_{\max}} L^3 \exp(-L) dL.$$

These errors are illustrated as bands in fig. 12. When making the fit these systematic errors are added in quadrature to the statistical errors from the Monte Carlo integration.

From fig. 12 it is clear that for $L \lesssim 7$ the sub-leading corrections start to become important. It is also clear that for $L \gtrsim 12$ the statistical errors start to increase significantly[†]. Thus we choose the fit range $7.1 < L < 12.1$. Fitting a constant in this range

[†]For even larger L the phase-space limitation imposed by the invariant mass cut-off becomes clearly noticeable.

gives the following results,

$$\begin{aligned}\mathcal{B}_{C_F,1} &= 2.95 \pm 0.27 \pm 0.11, \\ \mathcal{B}_{C_A,1} &= 1.855 \pm 0.081 \pm 0.093, \\ \mathcal{B}_{T_F,1} &= -1.255 \pm 0.022 \pm 0.010.\end{aligned}$$

where the first error is from the fit and the second from the maximal variation when varying the upper and lower limits for the fit by ± 1 .

From these results we can now get the NNLL term \mathcal{G}_{21} in the order a^2 contribution to $\ln R$,

$$\ln R = [\mathcal{G}_{12}L^2 + \mathcal{G}_{11}L] a + [\mathcal{G}_{23}L^3 + \mathcal{G}_{22}L^2 + \mathcal{G}_{21}L] a^2 + \dots$$

For the C_A and T_F parts these are just the same as the $\mathcal{B}_{i,1}$ but for the C_F part one has to subtract the contribution coming from the expansion of the exponent and the different normalisation used in Eq. (116), $(\pi^2 - 3)/4$. Adding the errors in quadrature and writing the result as

$$\mathcal{G}_{21} = \mathcal{G}_{\beta_0,1}C_F\beta_0 + \mathcal{G}_{C_F,1}C_F^2 + \mathcal{G}_{C_A,1}C_AC_F$$

we get

$$\begin{aligned}\mathcal{G}_{C_F,1} &= 1.23 \pm 0.29, \\ \mathcal{G}_{C_A,1} &= -1.60 \pm 0.14, \\ \mathcal{G}_{\beta_0,1} &= 3.766 \pm 0.070.\end{aligned}$$

These results can be compared with eq. (107) where

$$\begin{aligned}\mathcal{G}_{C_F,1} &\simeq 0.13, \\ \mathcal{G}_{C_A,1} &\simeq -0.73, \\ \mathcal{G}_{\beta_0,1} &= 3.75,\end{aligned}$$

in order to examine to what accuracy the DGE generates the sub-leading logs. The coefficient which is directly calculated in our approach is $\mathcal{G}_{\beta_0,1}$. In this case the agreement is very good. As expected, the other coefficients which are generated by the exponentiation do not agree. It is encouraging, however, that their values are smaller and that they have the correct signs. Thus, including the corresponding terms at NNLO and beyond is certainly an improvement.

For easy comparison with earlier results [6, 52, 44] we also write the result in the expansion

$$\ln R = [G_{12}L^2 + G_{11}L] a/2 + [G_{23}L^3 + G_{22}L^2 + G_{21}L] a^2/4 + \dots,$$

with $G_{21} = G_{T_F,1} + G_{C_F,1} + G_{C_A,1}$. Our results (for $N_F = 5$) are then given by

$$\begin{aligned}G_{C_F,1} &= 9 \pm 2, \\ G_{C_A,1} &= 30 \pm 2, \\ G_{T_F,1} &= -16.7 \pm 0.3.\end{aligned}$$

The result for the sum $G_{21} = 22 \pm 3$ agrees within errors with earlier results, but the results for the colour factors C_A and T_F are significantly different [44]. The reason for these discrepancies can probably be found in the different ranges in L used for the fit, namely $7.1 < L < 12.1$ and $3.1 < L < 6.7$ respectively.

References

- [1] M. Beneke, Phys. Rep. **317** (1999) 1, [hep-ph/9807443].
- [2] G.P. Korchemsky and G. Sterman, *Nucl. Phys.* **B437** (1995) 415.
- [3] Yu.L. Dokshitzer and B.R. Webber, *Phys. Lett.* **B404** (1997) 321.
- [4] M. Beneke and V. M. Braun, *Nucl. Phys. B* **454** (1995) 253, [hep-ph/9506452].
- [5] G. Sterman and S. Weinberg, *Phys. Rev. Lett.* **39** (1977) 1436.
- [6] S. Catani, L. Trentadue, G. Turnock and B.R. Webber, *Nucl. Phys.* **B407** (1993) 3; *Phys. Lett.* **B263** (1991) 491.
- [7] H. Contopanagos, E. Laenen and G. Sterman, *Nucl. Phys.* **B484** (1997) 303, [hep-ph/9604313].
- [8] S. Catani and B. R. Webber, *Phys. Lett. B* **427** (1998) 377 [hep-ph/9801350].
- [9] S. Catani, G. Turnock and B. R. Webber, *Phys. Lett. B* **295** (1992) 269; Y. L. Dokshitzer, A. Lucenti, G. Marchesini and G. P. Salam, *JHEP* **9801** (1998) 011 [hep-ph/9801324].
- [10] R.K. Ellis, D.A. Ross and A.E. Terrano, *Nucl. Phys.* **B178** (1981) 421; Z. Kunszt, P. Nason, *QCD, in Z Physics at LEP 1*, vol. 1, p. 373, Eds. G. Altarelli, R. Kleiss, and C. Verzegnassi (1989).
- [11] S. Catani and M.H. Seymour, *Phys. Lett.* **B378** (1996) 287; *Nucl. Phys.* **B485** (1997) 291; <http://hepwww.rl.ac.uk/theory/seymour/nlo/>
- [12] E. Gardi and G. Grunberg, *JHEP* **9911** (1999) 016, [hep-ph/9908458].
- [13] S.J. Brodsky, G.P. Lepage and P.B. Mackenzie, *Phys. Rev.* **D28** (1983) 228; G.P. Lepage and P.B. Mackenzie, *Phys. Rev.* **D48** (1993) 2250.
- [14] S. J. Brodsky, E. Gardi, G. Grunberg and J. Rathsman, *Disentangling running coupling and conformal effects in QCD*, to appear in *Phys. Rev. D*, [hep-ph/0002065].
- [15] S. Catani, G. Marchesini and B.R. Webber, *Nucl. Phys.* **B349** (1991) 635.
- [16] G. Corcella *et al.*, *JHEP* **0101** (2001) 010 [hep-ph/0011363].

- [17] T. Sjöstrand, P. Eden, C. Friberg, L. Lönnblad, G. Miu, S. Mrenna and E. Norrbin, hep-ph/0010017.
- [18] A. V. Manohar and M. B. Wise, Phys. Lett. **B344** (1995) 407 [hep-ph/9406392].
- [19] B. R. Webber, Phys. Lett. **B339** (1994) 148, [hep-ph/9408222].
- [20] Yu.L. Dokshitzer and B.R. Webber, *Phys. Lett.* **B352** (1995) 451.
- [21] R. Akhoury and V. I. Zakharov, *Phys. Lett.* **B357** (1995) 646, [hep-ph/9504248].
- [22] Yu.L. Dokshitzer, G. Marchesini and B.R. Webber, *Nucl. Phys.* **B469** (1996) 93.
- [23] G.P. Korchemsky and G. Sterman, 30th Rencontres de Moriond, *QCD and high energy hadronic interactions*, Les-Arcs, Savoie, France, 18-25 March, 1995. ed. J. Tran Thanh Van (Editions Frontieres, Gif-sur-Yvette, 1995), p.383, [hep-ph/9505391]
- [24] G. P. Korchemsky, *Shape functions and power-corrections to the event shapes*, hep-ph/9806537.
- [25] G. P. Korchemsky and G. Sterman, *Nucl. Phys.* **B555** (1999) 335, [hep-ph/9902341].
- [26] G. P. Korchemsky and S. Tafat, JHEP **0010** (2000) 010, [hep-ph/0007005].
- [27] E. Gardi, JHEP **0004** (2000) 030, [hep-ph/0003179].
- [28] P. Nason and M.H. Seymour, *Nucl. Phys.* **B454** (1995) 291.
- [29] L.S. Brown and L.G. Yaffe, *Phys. Rev.* **D45** (1992) 398; L.S. Brown, L.G. Yaffe and C. Zhai, *Phys. Rev.* **D46** (1992) 4712.
- [30] M. Beneke, *Nucl.Phys.* **B405** (1993) 424.
- [31] G. Grunberg, *Phys. Lett.* **B304** (1993) 183; see also *Quantum Field Theoretic Aspects of High Energy Physics*, Kyffhauser, Germany, September 1993.
- [32] Yu.L. Dokshitzer, A. Lucenti, G. Marchesini and G.P. Salam, *Nucl. Phys.* **B511** (1998) 396; *JHEP* **05** (1998) 003.
- [33] M. Dasgupta, L. Magnea and G. Smye, JHEP **9911** (1999) 025, [hep-ph/9911316]; G. E. Smye, *On the 1/Q correction to the C-parameter at two loops*, hep-ph/0101323.
- [34] J. Ellis, E. Gardi, M. Karliner and M. A. Samuel, Phys. Lett. B **366** (1996) 268 [hep-ph/9509312].
- [35] G. Grunberg, *Phys. Lett.* **B372** (1996) 121. **B380** (1996) 141.
- [36] E. Gardi and M. Karliner, Nucl. Phys. **B529** (1998) 383, [hep-ph/9802218]; E. Gardi, G. Grunberg and M. Karliner, JHEP **9807** (1998) 007, [hep-ph/9806462].
- [37] A. Vogt, hep-ph/0010146; Phys. Lett. **B497** (2001) 228.

- [38] S. Kluth, Ph.D. thesis (1995), *Studies of QCD using event-shape observables in e^+e^- annihilation at the Z^0 energy*.
- [39] B. R. Webber, JHEP **9810** (1998) 012, [hep-ph/9805484].
- [40] S. J. Burby and C. J. Maxwell, hep-ph/0011203.
- [41] A. Banfi, Y. L. Dokshitzer, G. Marchesini and G. Zanderighi, hep-ph/0010267; A. Banfi, Y. L. Dokshitzer, G. Marchesini and G. Zanderighi, JHEP **0103** (2001) 007, [hep-ph/0101205].
- [42] G. P. Salam and D. Wicke, “Hadron masses and power corrections to event shapes,” hep-ph/0102343.
- [43] E. Gardi, talk at the 35 Rencontres des Moriond, Les Arcs, France, 18-22 March 2000, http://moriond.in2p3.fr/QCD00/transparencies/4_wednesday/pm/gardi/
- [44] R. Akers *et al.* [OPAL Collaboration], Z. Phys. C **68** (1995) 519.
- [45] W. Braunschweig *et al.* [TASSO Collaboration], Z. Phys. C **47** (1990) 187.
- [46] P. A. Movilla Fernandez, O. Biebel, S. Bethke, S. Kluth and P. Pfeifenschneider [JADE Collaboration], Eur. Phys. J. C **1** (1998) 461 [hep-ex/9708034].
- [47] Y. K. Li *et al.* [AMY Collaboration], Phys. Rev. D **41** (1990) 2675.
- [48] R. Barate *et al.* [ALEPH Collaboration], Phys. Rept. **294** (1998) 1.
- [49] P. Abreu *et al.* [DELPHI Collaboration], Eur. Phys. J. C **14** (2000) 557 [hep-ex/0002026].
- [50] B. Adeva *et al.* [L3 Collaboration], Z. Phys. C **55** (1992) 39.
- [51] G. S. Abrams *et al.* [MARK-II Collaboration], Phys. Rev. Lett. **63** (1989) 1558.
- [52] P. D. Acton *et al.* [OPAL Collaboration], Z. Phys. C **59** (1993) 1; see also [38].
- [53] K. Abe *et al.* [SLD Collaboration], Phys. Rev. D **51** (1995) 962 [hep-ex/9501003].
- [54] D. Buskulic *et al.* [ALEPH Collaboration], Z. Phys. C **73** (1997) 409.
- [55] P. Abreu *et al.* [DELPHI Collaboration], Phys. Lett. B **456** (1999) 322.
- [56] G. Alexander *et al.* [OPAL Collaboration], Z. Phys. C **72** (1996) 191.
- [57] ALEPH Collaboration, “QCD studies with $e^+ e^-$ annihilation data from 130-GeV to 172-GeV”, CERN-OPEN-99-323, *Prepared for International Europhysics Conference on High-Energy Physics (HEP 97), Jerusalem, Israel, 19-26 Aug 1997*.
- [58] K. Ackerstaff *et al.* [OPAL Collaboration], Z. Phys. C **75** (1997) 193.

- [59] M. Acciarri *et al.* [L3 Collaboration], Phys. Lett. B **404** (1997) 390.
- [60] G. Abbiendi *et al.* [OPAL Collaboration], Eur. Phys. J. C **16**, 185 (2000) [hep-ex/0002012].
- [61] ALEPH Collaboration, “Preliminary ALEPH results at 183-GeV”, *Prepared for International Europhysics Conference on High-Energy Physics (HEP 97), Jerusalem, Israel, 19-26 Aug 1997.*